

Development of EMAT Sensors for Corrosion Mapping of UNGP Using ILI Tools

Project Final Report Public Version

P. Bondurant
G. Nino

December 2019

Prepared for

U.S. Department of Transportation
Pipeline and Hazardous Materials Safety Administration

Contract Number

DTPH5616T00002



Quest Integrated, LLC.
19823 58th Place S, Suite 200
Kent, Washington 98032
(253) 872-9500

PROJECT OBJECTIVE AND SCOPE

Development of a bench-scale electromagnetic acoustic transducer (EMAT) sensor that can be used to assess the wall thickness of small diameter unpiggable pipelines containing reduced diameter fittings and other restricting features.

This objective implies improved EMAT functionality in relatively thin walls, 0.25" to 0.5" with further thinning due to corrosion. Corrosion can be particularly problematic for both EMAT and traditional ultrasound wall thickness measurements due to the scattering of the ultrasonic energy. The better the EMAT sensor is for thickness measurement on corroded surface, the better the POD will be for the final fielded instrument and the less data interpretation required.

The ultimate commercial system will be independent of the specific locomotion method. The initial commercial embodiment will likely be a tethered or robotic vehicle.

Additional funding was allocated to the program for a second phase which allowed integration of the EMAT wall sensors into a tethered robot

SUMMARY

The program essentially executed into two phases. The first phase focused on the development of the sensor and a bench scale EMAT system (deliverables 1 through 6) and the second phase focused (deliverables 10 through 17) on integrating the new EMAT sensor into a field deployable robot.

The EMAT sensor developed during this project dramatically decreases the sensor footprint area by a factor of 16 *without a reduction in sensitivity*. In addition, the attraction force between the sensor and the pipe wall is significantly reduced which reduces the frictional on the wear pads and reduces the power required to move the sensor across the surface. A patent has been submitted for the new EMAT sensor design. The sensor has application for both wall loss and angle beam measurements. This project focused on robotic or remote applications; however, the sensor is also useful for handheld applications. Most field inspectors who use EMAT sensors would prefer to use our version of the sensor due to its reduced surface attraction and small measurement footprint.

A small measurement footprint is what is necessary to determine the minimum remaining wall in areas of corrosion. The larger the measurement footprint of a sensor, the larger the diameter the corrosion needs to be to obtain an ultrasonic reflection. If the measurement footprint of the sensor is a one square inch, it will not be able to sense the minimum remaining wall thickness in the bottom of a small pits. A sensor footprint of 0.25" has a much higher probability of obtaining the remaining wall.

The original goal of the program was to develop a remotely deployable EMAT sensor optimized for corrosion mapping. This has been accomplished. Not only an optimized sensor was developed but also compact electronics necessary for operating the sensor were developed. The electronics, when paired with the sensor, minimized the ring down of the system to improve the ability of the system to receive the first backwall echo. This further optimizes the system for the measuring remaining wall thickness in areas of corrosion.

The second phase of the program integrates the corrosion optimized EMAT system into a semi-custom scanner robot for remote inspection in pipelines. The system was tested in house and on the field to demonstrate its maturity and performance. Results from that testing activity are presented on this document.

This report summarizes the work completed on this program. The report is divided into five sections: sensor development, bench-scale demonstration, robot and system integration development, shop testing, and field testing.

EMAT SENSOR DEVELOPMENT

Ultimately the performance of a fielded system can only be as good as the basic sensor, so the focus here is to briefly describe the problem from the sensor perspective. We identified several considerations for the design of the sensor to perform in thin walls with corrosion.

1. OD Surface Ultrasonic Scattering
2. Sensor ring-down/dead time
3. ID coupling
4. Sensor size versus corrosion topology

OD Surface Scattering/Ring-Down

One of the first aspects to consider during the development of an ultrasound-based inspection technology is the pipe surface topology. A rough surface can affect the acoustic responses in terms of signal scattering and ring-down. These issues are illustrated in Figure 1. The left side of the figure is an EMAT A-Scan from a thicker wall riser pipe section (roughly 29 mm), while the EMAT A-Scan on the right is an area where only one reflection from the OD wall was received. This is representative of what will happen if there is OD corrosion present. Instead of the ultrasonic sound energy reflecting directly from the OD surface back to the EMAT sensor, it scatters, reducing the probability of receiving multiple echoes. Worst case scenario is that the sensor does not receive any echo and a measurement cannot be made. The other issue illustrated in Figure 1 is the dead time or ring-down associated with the sensor. From the A-Scan on the right, one can estimate that the dead time is approximately 8 μs . The electronics driving this sensor was designed for thicker walls and for use in guided wave applications where the dead time is not of significant concern. However, for walls that are in the target range of 0.25" to 0.5", not including corrosion, this is a problem. For reference, the first reflection from the 0.4" wall will be around 6.7 μs and 2.0 μs for a 0.1" thick wall. If there is only one reflection received from the OD, excessive dead time will completely mask the measurement. The sensor must rely on multiple reflections to make a measurement. Multiple reflections are easily obtained on non-corroded surfaces or surfaces where the corrosion topology variation is much larger than the sensor dimensions. The key point is that the sensors ability to make measurements in corroded areas is the key evaluation criteria for an EMAT sensor. Although the lack of measurements in a corroded area of a pipe is information, it does not provide the information necessary to make any critical decisions. Typical dead times for commercially available EMAT sensors are about 4 to 5 μs , so the first echo would not be detectable for wall thicknesses less than approximately 0.3", the first echo would begin to blend into the ring-down and one would have to rely on additional echoes to make the measurement. This is only slightly smaller than a typical pipe wall thickness. In a situation where there is significant wall loss the sensor can only report "no reading".

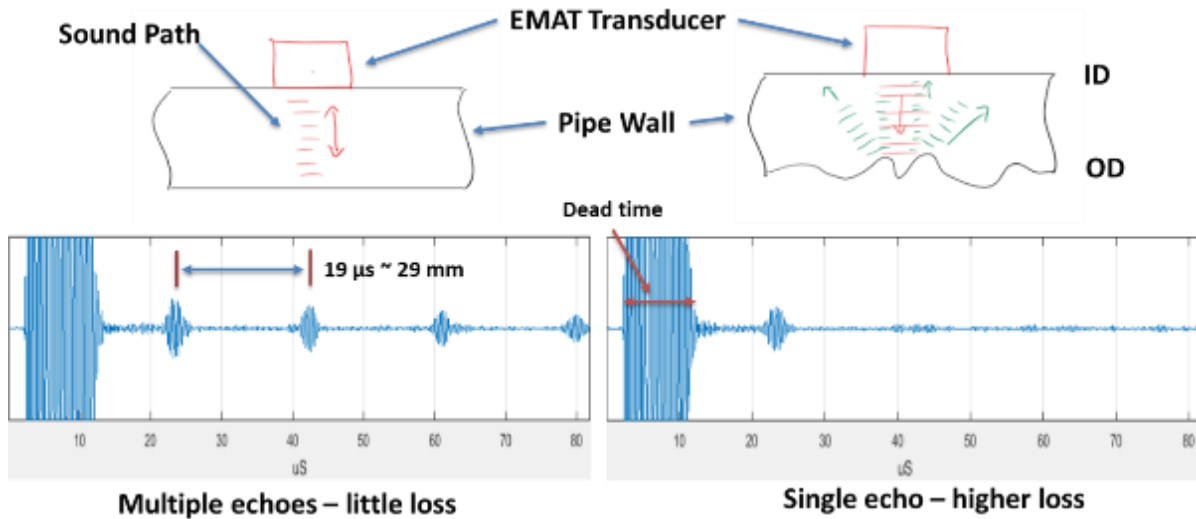


Figure 1 – EMAT A-Scan Responses for Two Different Scenarios: Clean Wall (left) and Corroded Wall (right)

ID Coupling

EMAT sensors create the ultrasonic signal in the pipe wall through the interaction of eddy currents in the pipe surface with a co-located static magnetic field. This transduction method provides the primary advantage of EMAT, ultrasound coupling liquids or gels are not required. The eddy currents are generated through inductive coupling from a radio frequency (RF) coil located in the EMAT sensor assembly. A magnet typically generates the static magnetic field. For send/receive topologies, the ultrasonic signal is proportional to the square of the static magnetic field and linearly with respect to the transmit coil current. The static magnetic field and induced RF current get smaller as the distance between the sensor and the surface increases. The typical lift-off range of an EMAT sensor is 2 mm, in real situations it can be larger. In certain situations, a magnetite film on the pipe surface can greatly enhance the signal strengths. Even without a signal enhancing deposit, the sensor can see through a reasonable amount of scale. The complication is the presence of ID corrosion, if it is deep enough the effective lift-off increases, and sensor reaches a point where the A-Scan signal is lost, and the system will report “no reading”. The mechanical design of the tool is tasked with keeping the sensor reliably on the surface to minimize lift-off and lift-off variations. To minimize ID coupling problems, the sensor must operate at maximum static magnetic field strength and maximum RF current levels. Also because of ID corrosion, the probability of multiple wall return echoes is lower so the minimization of the dead time is important for this situation as well.

Sensor Size Versus Corrosion Topology

One method to mitigate the lower amplitude signals caused by scattering is to reduce the size of the EMAT sensor. Figure 2 illustrates the situation. A large transducer may span a significant variation in the corrosion surface slope where the useful reflected ultrasonic energy is only from the corrosion peaks where the ID and OD surfaces are near parallel. The sloped areas reflect

energy away from the useful measurement direction. This scattering causes numerous issues; different path lengths causing blurring, mode conversion, shear wave polarization rotation, missed reflected energy, all of which reduce the reflected signal level and cause a blurring of return echoes. However, if the same energy can be focused in a smaller area, the percentage of the corrosion peak width (where it is the deepest) is a larger percentage of the transducer area increasing the probability of a good measurement. *The primary focus of a wall thickness tool is to obtain the minimum wall thickness.* EMAT's have traditionally required a large area to obtain good signal-to-noise ratios where the magnet diameter sets the area. The density of the magnetic field is limited by the magnets that are commercially available. Larger area transducers may be useful if the corrosion depth peaks are relatively the same height.

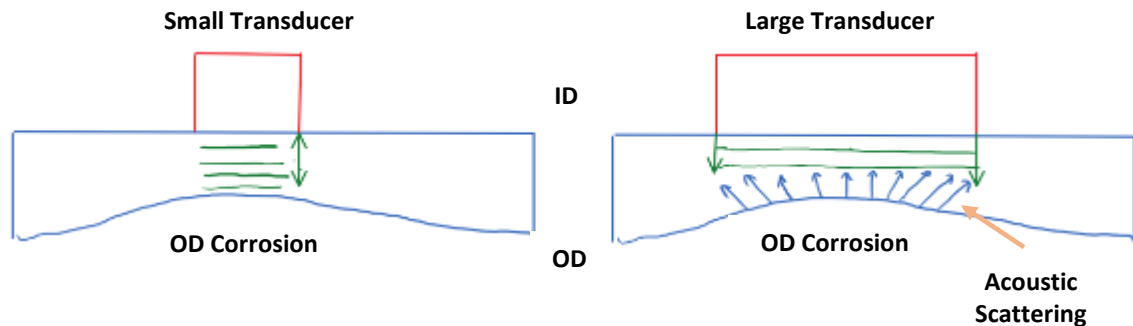


Figure 2 – EMAT Transducer Size Relative to the Corrosion Topology

Sensor Design

The development of an EMAT sensor is a multi-discipline problem. The design of a system requires optimization of the static magnet used for the bias field, attention to the acoustics, understanding of the electromagnetics to optimize the design of the RF coil, electrical design capability for a high-power transmitter and low-level receive capability, as well as an understanding of various signal processing methods to extract wall thickness information from the received signals. Transmit voltages can be about 1000 volts and the received signals are about 10 microvolts. For thin walls, the receive signal occurs within a few microseconds after the transmit signal ends further challenging the design. So, as stated earlier, dead-time (or ring-down) reduction was one of the stated goals of this project. The complex nature of the design and optimization process is likely why EMAT's are not as prevalent in the industry as compared to piezo-based ultrasound transducers even though they have some unique capability, specifically couplant-free and direct shear wave generation. There is no single book or article that provides a detailed analysis of all aspects of an EMAT design.

On this project, we considered the Lorentz style EMAT transducer configuration. This design works on both magnetic and non-magnetic conductors and our experience has been that they are more sensitive for a given magnet size. They are also more compact. The alternative is magnetostriction based where the transduction efficiency can be a significant function of the horizontal magnetic field strength.

All aspects of the sensor design were considered which included 3D analysis of the magnetic fields, RF coil design using electromagnetic field simulations, and circuit design analysis of the transmit, diplexor and receiver front end. Several versions of the electronics and sensor were fabricated and tested with iterative improvements along the way. A patent application has been submitted for the design.

The latest version of our new EMAT sensor has a sensor footprint (sensing area) of $\frac{1}{4}$ " , roughly $\frac{1}{16}$ " the sensing area of a commercial EMAT wall loss transducer. It has the same sensitivity as a commercial sensor. The Ascan amplitude is the same on a flat plate when compared to a commercial EMAT sensor with a 1" sensing diameter. In addition, the reduction in sensitivity with lift off is the same between both sensors. We believe that this is a significant break-through. Our sensor also has less signal interference just after the ring down portion of the Ascan waveform. This helps distinguish the first OD return echo in difficult to measure situations. The other advantage with the new sensor is the significant reduction in the attraction force between the wall and sensor. This makes the sensor easier to use manually and easier to integrate for automated applications and reduces the wear.

EMAT Sensor Testing

Several handheld versions of the EMAT sensors were fabricated to evaluate their performance based on lift-off and various surfaces conditions among others. Initially, the sensors were tested on two corrosion samples to simulate real piping conditions. The first has small surface pitting on both the ID and OD surfaces. This is typically a rare situation because usually the inner and outer surfaces are subjected to different environments and are not likely to corrode in the same place from the same mechanism. This $\sim\frac{1}{4}$ " wall sample is 6" diameter and is a severe test case that is difficult to measure using either EMAT or UT.

An EMAT A-Scan of the sample is shown in Figure 3 where 3 reflections can be observed. Other places on the surface would show no reflections or maybe only 1 reflection. The scale at the bottom is in microseconds and the actual thickness of the sample is 0.285". The EMAT electronics (commercial system) was damped to provide the short, $< 4 \mu\text{s}$ ring-down and the RF coil only has a 0.3 mm lift-off from the surface. Even though, we could obtain some useable reflections with our $\frac{1}{4}$ " sensor, a larger 1" sensor produced responses a bit more reliable. It was concluded that the larger area sensor covered enough area that there were sufficient non-corroded areas to obtain a signal however, this does not identify the deepest pit. We should point out that the A-Scan shown in Figure 3 was produced by our original $\frac{1}{4}$ " sensor, subsequent versions of the sensor would be improved and would like provide similar performance to the 1" sensor. The main point here is that there are surfaces that are difficult to measure regardless the technology.



Figure 3 – EMAT A-Scan of 0.285” (7.2mm) Thick Sample with Severe Corrosion on Both ID and OD.

Another sample has simulated corrosion on the ID and it can be observed in Figure 4. The EMAT sensors were tested from the OD of the sample. In this case, the topology of the corrosion is typically larger than the sensor footprint, so as expected, the sensors would receive thickness echoes from the bottoms of the corrosion pits. A qualitative comparison was made between the 1/4”, 3/8” sensors and a commercial sensor with a 1” footprint. EMAT A-Scans for these sensors at two different locations are shown in Figure 5. Clearly both smaller spot size sensors did a much better of finding pit bottoms as demonstrated by higher amplitude return echoes and multiple echoes. They found more locations in the sample with useable return echoes and when the same locations were tested with the large footprint commercial sensor; either a reflection was not found, or it was much weaker. It should also be noted that the commercial sensor has an artifact in the A-Scan. This could cause confusion in any post data analysis. Clearly the smaller footprint sensors have the capability of providing an improved Probability of Detection (POD).



Figure 4. Simulated Corrosion Sample

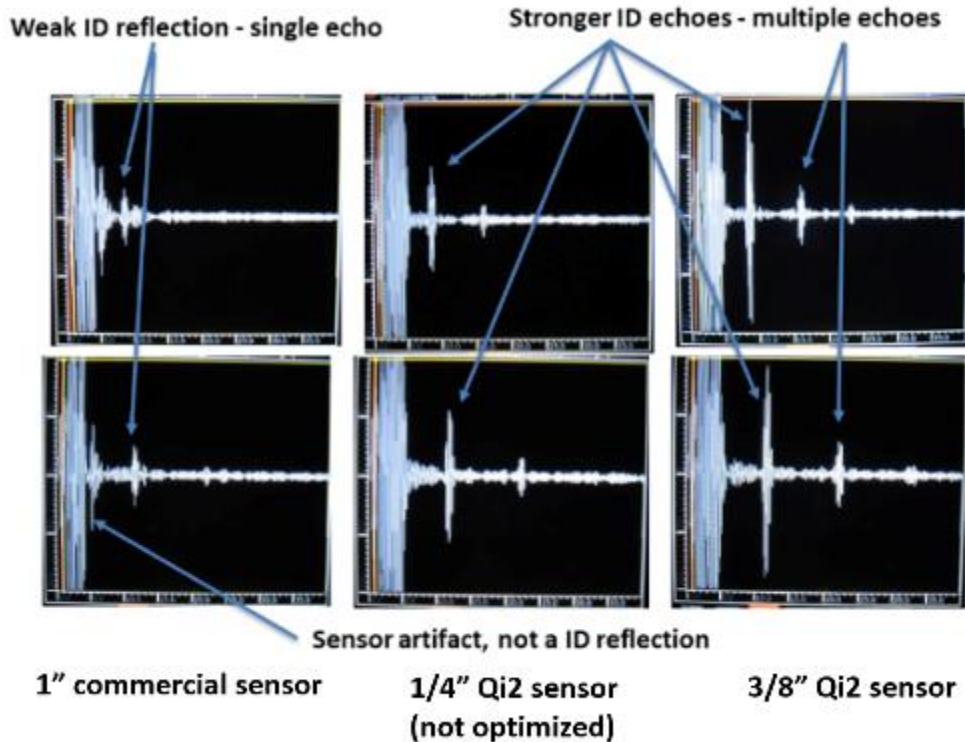


Figure 5. EMAT A-Scan Results from Two Pit Bottom That Could Be Seen by a 1" Commercial EMAT Sensor.
 Note: The gain was the same for all three images.

For demonstration purposes, a metal test sample was fabricated with a 3/8" wide flat bottom slot and a series of increasingly smaller round end-mill slots. The 1" commercial sensor could not really resolve any of the features while the 1/4" sensor could clearly resolve the bottom of the 3/8" slot and clearly see reflections from the bottoms of all but the smallest of the end-mill slot. The smallest round end-mill slot was approximately 4 mm wide at the surface and 1.25 mm deep at the apex. It was just visually notable in the A-scan.

More testing results from the optimized sensors are shown in the following sections.

The oscilloscope screen shot in Figure 6 shows the A-Scan from a 3/16" thick sample using the optimized sensor and electronics. This uses a single cycle pulse from the pulser and demonstrates a wide bandwidth signal. The first return echo from the sample is clearly resolved. Of course, the multiple echoes show minimal decay because only a small amount of energy is lost at each interface reflection due to the large acoustic impedance mismatch and the clean surfaces.

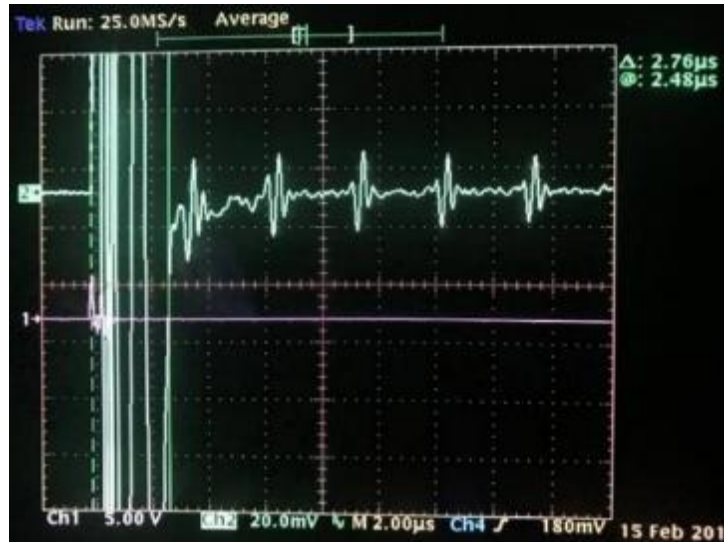


Figure 6. A-Scan from 3/16" Thick Sample Using the Optimized 1/4" Sensor

BENCH-SCALE EMAT SYSTEM

The next step after developing the EMAT sensors was to design and build a bench-scale device to deploy the sensors inside a tubular structure. A mechanical design for a tool that was based on 4 small-footprint EMAT sensors was envisioned. To provide a 100% coverage, the sensors were rotated. Once the system was fabricated, it was tested inside a pipe with manufactured flaws.

Design

A Solidworks™ design of the bench-scale sensor module is shown in Figure 7. The concept selected was more advanced than a bench-scale version that was originally proposed. The bench-scale device has two primary components: (i) the rotating sensor assembly, and (ii) the fixed drive assembly. The sensor assembly was positioned axially between two halves of the drive assembly. The extended wheel on the drive assembly prevents the overall tool from rotating.

Each of the four sensor carriers contains a single 3/8" EMAT sensor, so rotating at a constant rate using a fixed axial speed provides 100% coverage. Originally, we planned to have more than one EMAT sensor per carrier but decided it would have been too complicated to package the electronics at this stage of development. Each carrier was equipped with four steel ball transfers positioned to reduce contact and friction between the pipe wall and carrier body. Two metal shoes with threaded pivot pins were attached on each end of the carrier for easy access and mobility within the sensor assembly. The axial shape of the carrier has the proper curvature and size to accommodate 1D bends and intersecting pipes. One side of the carrier assembly (labelled leading edge) is sloped to protect the sensor sled from protrusions on the pipe wall. Essentially, the carrier will pull away from the surface along with the sensor sled if there is a protrusion.

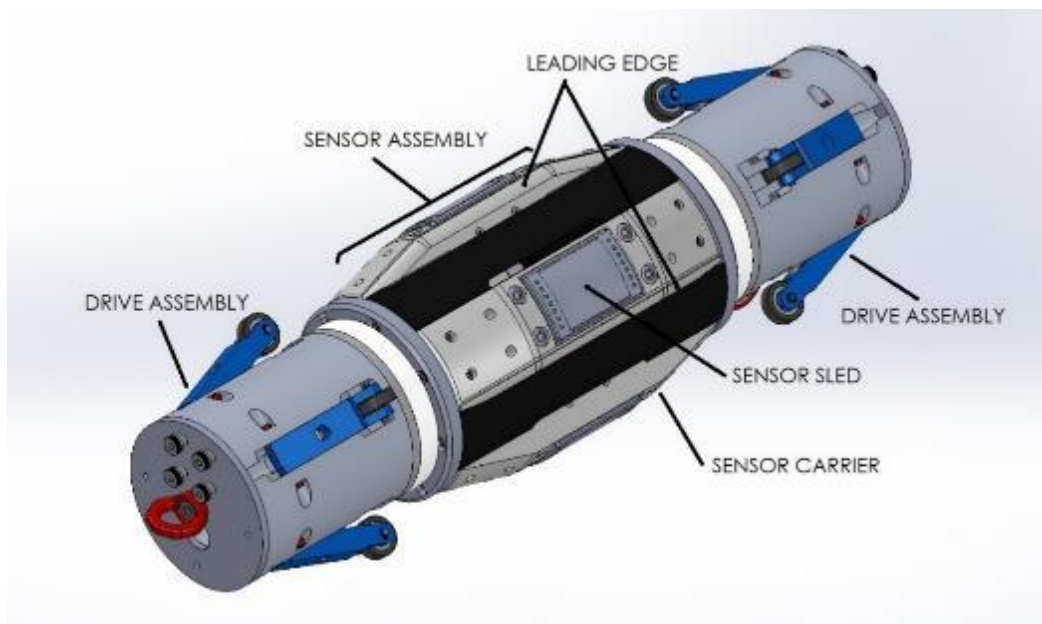


Figure 7. Bench-scale EMAT Sensor Module Design

The four sensor carriers were mounted equally spaced around the circumference of the sensor assembly. Each carrier fits in a hollow machined body with each carrier extended using springs. Two end caps were used to limit their radial extension of the carriers while allowing each to pivot independently. This allows the carriers to conform to the walls of non-circular pipes. One end cap has a large output gear and slip ring that was attached to the non-rotating drive assembly. Because the electronics and all processing were done within the rotation section of the module, the wire routing between the electronics and EMAT sensor is short and the slipping only needed to accommodate the power and ethernet connections.

The drive assembly has four tension-adjustable, independent wheels to grip the pipe wall. These prevent tool rotation. The wheel assembly has limited radial travel so that one can span a Y-joint without getting stuck. A motor drives a small input gear that spins the sensor assembly via the larger output gear attached to the carrier end caps. An additional encoder was used to record the axial motion. Each end of the drive assembly is equipped with a lifting eye to attach a cable or some other means of locomotion to move the sensor module through the pipe.

The primary purpose of the sensor sled design is to keep the RF (radio frequency) coil in the EMAT sensor flush with the surface and keep the bias magnet near the surface while at the same time minimize wear and friction. Ultimately it also must be impervious to protrusions such as weld beads or slag. The sensor carrier/sled combination must accommodate changes in sensor module centering and deformity in the pipe. As discussed earlier, the carrier upon which the sensor sled is mounted provides pitch and yaw variability. The sensor sled allows the EMAT sensor to extend radially as necessary. Compliant material between the bias magnet and the RF coil provide some pipe surface accommodation.

Regarding hardware, several modifications to the electronics and processing were implemented in Qi2 thick-wall riser inspection tool ($WT \geq 0.5''$) for testing. In addition, firmware was also modified to implement required processing needs.

Fabrication and Assembly

The bench-scale device was fabricated and assembled as shown in Figure 8. It can be observed that the drive/centering mechanisms are mounted on each end of the rotating sensor/electronics assembly. The extendable arms with the black wheels are used for centering and the red wheel is the axial encoder. Figure 9 shows photos of the drive end of the module with and without the motor assembly installed. The power and ethernet cables to the electronics are also shown. An ethernet rated slip ring was used within the module to bring power, ethernet and encoder signals in and out of the rotating sensor modules.



Figure 8. Assembled Sensor Module.



Figure 9. Drive End of the Sensor Module with the Drive Motor Assembly Installed (right) and Without (left)

The assembled tool electronics, i.e. a four channel pulser, a receiver and ethernet communications boards, are shown in Figure 10. The photo on the left is the cylindrical card cage assembly the fits in the center of the rotating portion of the tool. The photo on the right is the card cage partially inserted into the sensor module before the slip ring and drive components are installed.

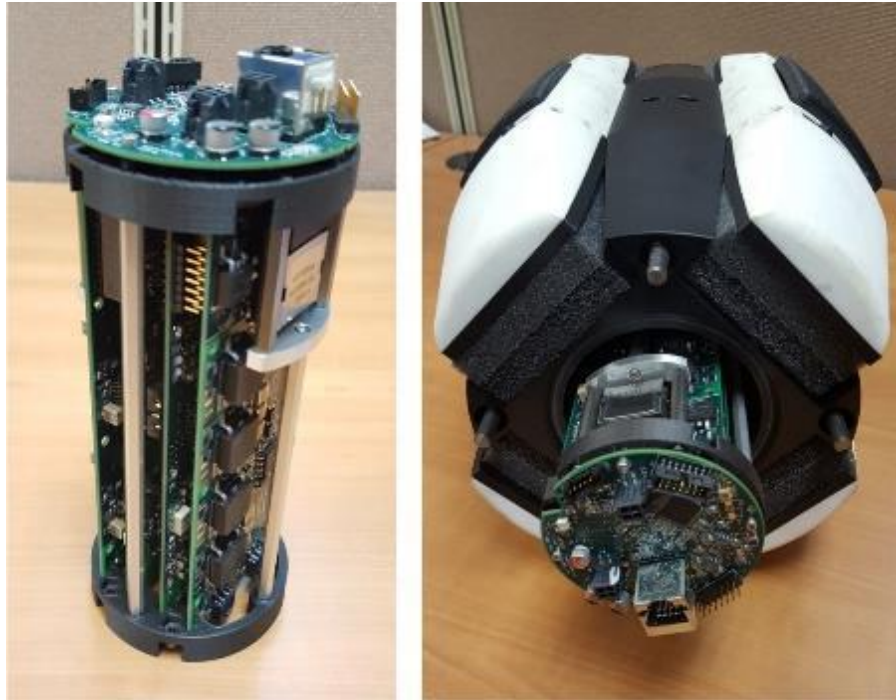


Figure 10. Custom EMAT Electronic Board Cage (left) and Partially Inserted Cage into The Rotating Sensor Module (right). Note the ethernet connector is protruding from the end.

Test Sample

A test sample was fabricated from a short section of 8" schedule 40 pipe with a nominal wall thickness of 0.322". The sample is shown in Figure 11. Note that all the machined flaws in the pipe present a curvature to the EMAT sensor as opposed to machined flaw samples that have an extended uniform wall thickness over an area that would be easy to measure and detect, if they are the same size or larger than the 3/8" or 1/4" sensor footprint.

In the case of the slots or flats, the bottoms of the flaws are uniform in wall thickness only along a line along the pipe axis. For the small radius flaws the minimum wall is at a point. Two different ball-end-mills (1/4" and 1/2" radius) were used to create the rounded flaws. Detection of these flaws is particularly difficult because the energy is deflected away from the sensor at every location along the flaw other than at the single point where the surface is tangent to the sensor. The measurement is further complicated by the fact that the acoustic signal is created along ID radius that diverges the beam and then hits a flaw bottom that further diverges and blurs the signals.



Figure 11. Fabricated Flaws – The Seam Is at The Bottom on The Top Photo and on The Top of The Bottom Photo

Bench Testing

The bench-scale prototype was tested on the pipe of Figure 11 as can be observed in Figure 12. As mentioned before, the bench-scale prototype was fabricated with 3/8" footprint sensors as opposed to the 1/4" sensors. In retrospect, we probably should have used the smaller sensor, however the larger footprint sensor had slightly better sensitivity and we wanted to test to see how well the device could rotate four sensors with the greater friction. An EMAT C-Scan of the pipe section is shown in Figure 13. The seam runs through the center of the scan. The height of the C-Scan is approximately 24" (the circumference of the pipe), so the spacing between the thin red stripe representing the thicker part of the pipe around the seam is spaced approximately 1" from the yellow stripe.



Figure 12. Test Setup with Bench EMAT Scanner Inserted

Note how thin the red stripe is, as well as the orange stripe between the yellow and red stripes. This demonstrates the high spatial resolution of the 3/8" sensor. The 2" long machine flats were clearly resolved. They appeared as different lengths because the tool's axial speed was not uniform. The end mill slots were also resolved. Note that the ends of the C-Scan are stepped due to the 4 individual sensors, which are offset circumferentially around the pipe ID.

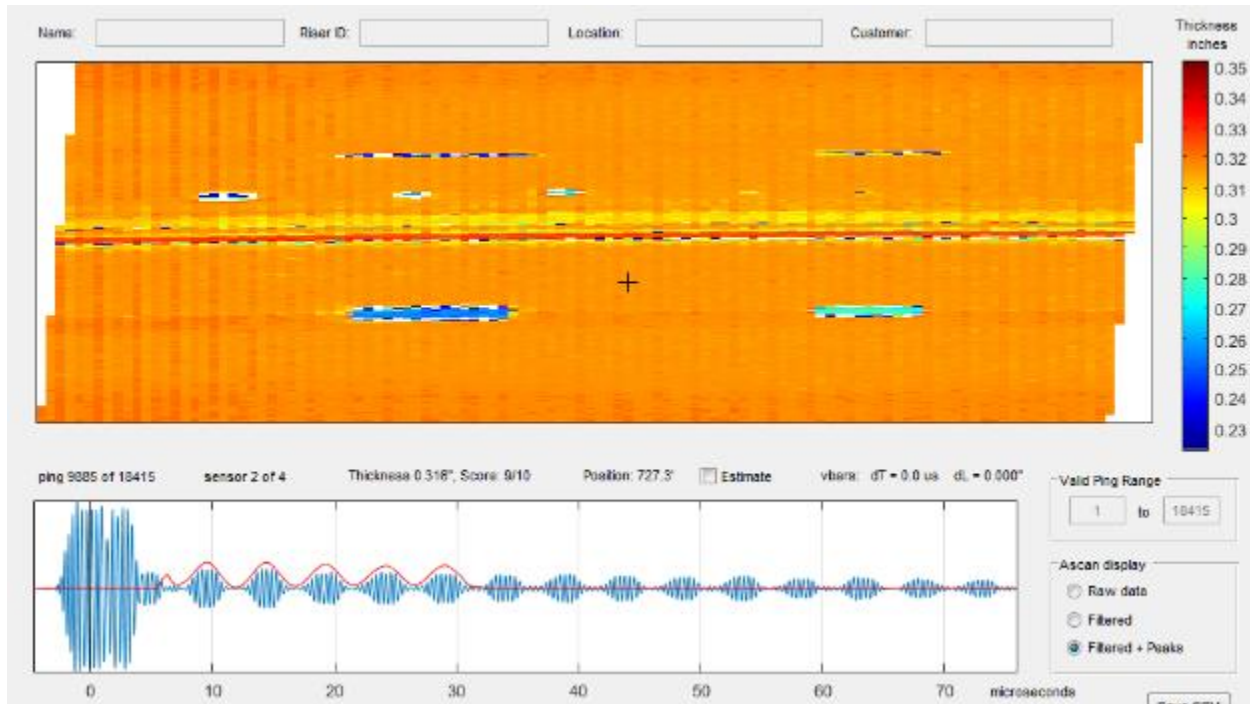


Figure 13. Pipe Section C-Scan and A-Scan Using Four 3/8" Footprint EMAT Sensors

The 1/2" square flats were also detected with some radius readings. The two deeper 1/2" round bottom holes were detected too. The four small 1/4" round bottom holes were not detected. However, their signature can be found in the data set as a reduction in signal amplitude. This could be used as a detection method to determine when the data analyst should review the A-Scan. Essentially the automated processing significantly reduces the amount of data that the analyst must review.

ROBOT AND SYSTEM INTEGRATION DEVELOPMENT

Once the EMAT/WT was successfully tested at the bench level (the first phase), a more robust platform for field testing was designed and fabricated (second phase). In consultation with Inuktun Services Ltd. (Eddyfi Technologies nowadays), a robot platform was selected, and a preliminary design was developed for the integration of this platform with an array of 1/4" EMAT sensors. The platform is based on the VT100 vertical crawler (Figure 14), which is capable of operating in 6" to 12" diameter pipe and can negotiate a 1.5D bend in pipes that 8" and larger in diameter.



Figure 14. Inuktun Services Ltd. VT100 Vertical Crawler

The specialized VT100 vertical crawler module provides centering within the pipe as well as superior traction for forward/backward motion. The EMAT sensors were mounted on a separated cart. This carrier was designed to first expand the sensors against the pipe wall and then to rotate the whole module during the scan process.

Conceptual Design

The conceptual EMAT cart design was sized for an 8" to 12" pipe. Larger pipes would require a scaled-up version of the expansion mechanism and a modified version of the EMAT sensor cart for the larger radii inner surface. The trailing electronics cart houses the power conversion and distribution, fiber optic terminations, video and communication electronics. A fiber optic and power umbilical connected the robot to a computer and power supply (base station). A sketch of the initial design is illustrated in Figure 15.

The selected robot platform supports Ethernet communication over a fiber optic-based umbilical and is equipped with multiple cameras and encoders. The robot will take the Ethernet packets from the EMAT communication board and convert them to an optical format for long-distance transmission over the umbilical. At the end of the umbilical (outside the pipe), another interface will convert the optical signals back into a standard 100baseTX format for connection to a laptop computer.

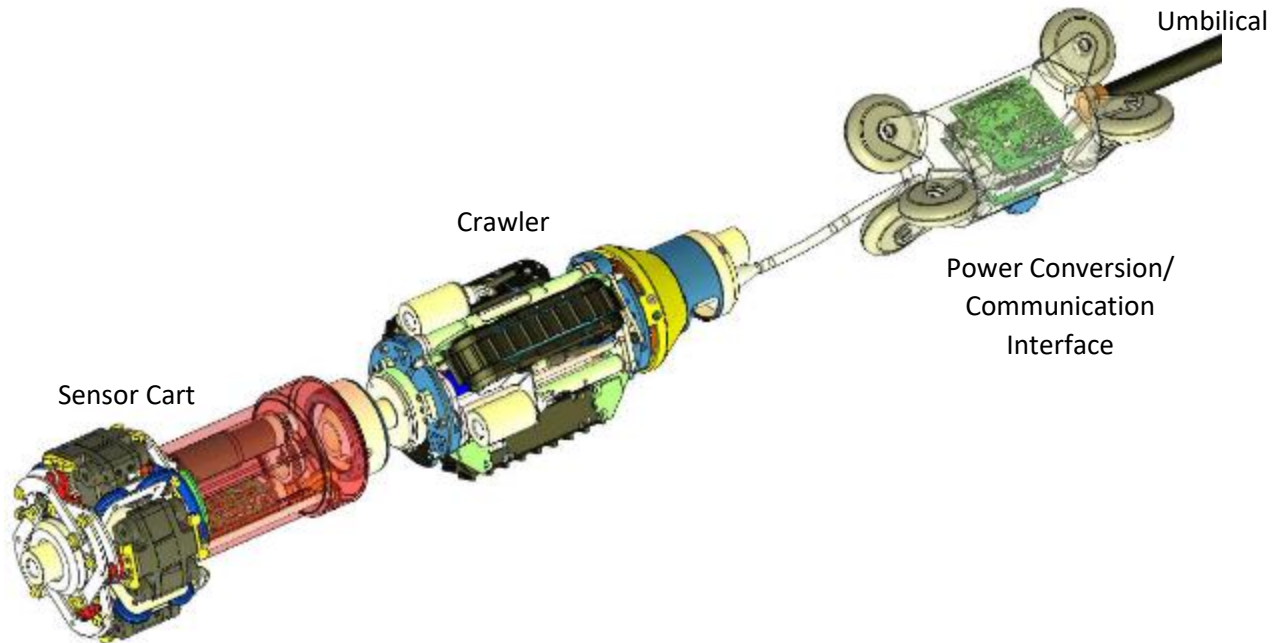


Figure 15. Initial Robot System Design Concept.

Preliminary Design

Further market research indicated that a final inspection tool should include a secondary sensor, such as pulsed eddy current (PEC), to augment the EMAT wall loss sensor. This provides a lower resolution wall loss measurement as well as a measurement of the internal surface of the pipe. This compliments the EMAT sensor, particularly in those situations where the inner pipe wall may be too rough to allow efficient coupling between the EMAT sensor and the pipe wall.

Based on the new information, the robot system was redesigned for integration of two PEC sensor within the sensor module along with the necessary space to house the associated electronics. It is important to note that due to the effort required to develop a smaller PEC sensor head, it was not integrated on this project as is not part of the contract. In addition, the redesigned provided better navigation of the sensor module through the bends. The goal is to attain as least PEC measurements in the bends. This design reduced the number of EMAT transducers from 4 to 2. The redesign is shown in Figure 16.

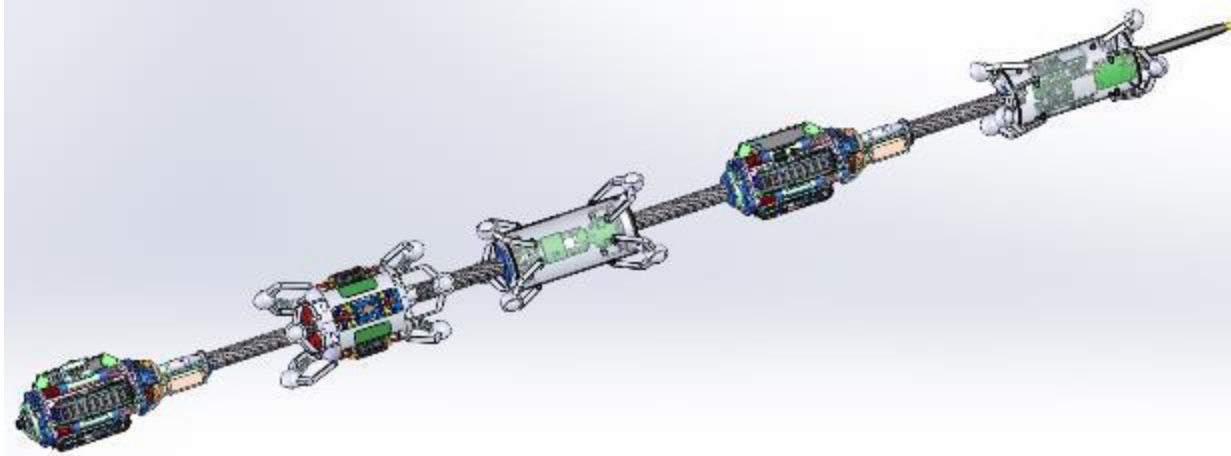


Figure 16. EMAT and PEC Crawler Concept

The modules are interconnected with electrical conductors running inside flexible springs. The crawler modules expand to the pipe walls to provide motive traction. The remaining modules are centered using spring loaded linkages and castor style rollers. The sensor electronics module and EMAT/PEC module rotate in unison – driven from a micro controlled motor contained inside the EMAT/PEC module. This eliminates the need for a slip ring between the electronics and the sensors. The EMAT/PEC module also contains a motor to expand and contract linkages which bring the sensors in contact/proximity to the pipe wall. A detailed view of the EMAT/PEC sensor module is illustrated in Figure 17.

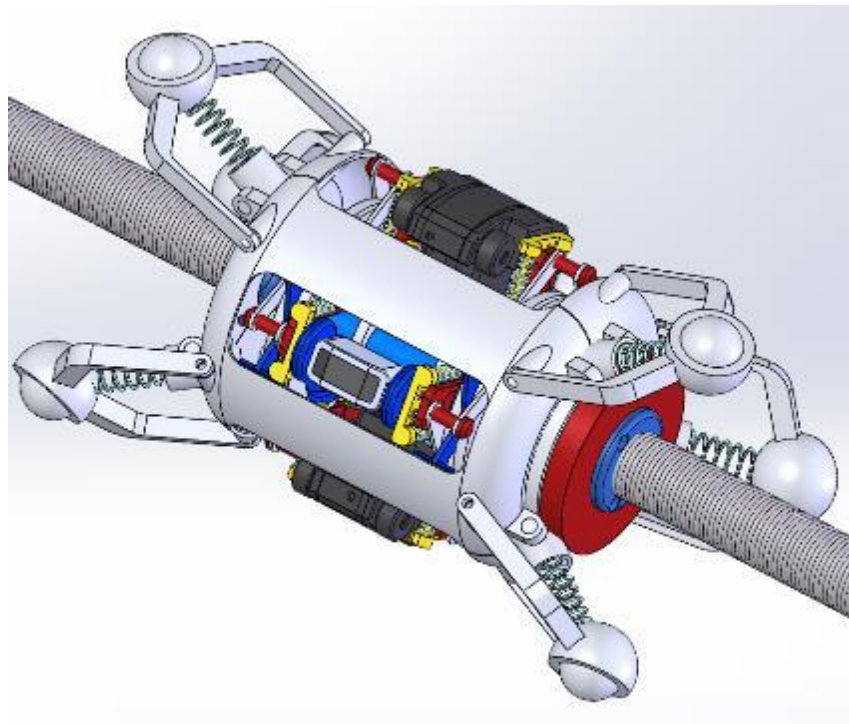


Figure 17. EMAT/PEC Sensor Module

Detailed Design and Fabrication

The EMAT/WT Robotic system design was further detailed, in particular the EMAT/PEC crawler mechanical design was improved. The resulting design for manufacturing is shown in Figure 18. In particular, the wheeled system on the vehicle and sensor electronics modules were updated to ensure a better ride and contact along the pipe. A detailed view of the sensor electronics module is depicted in Figure 19. The EMAT/PEC crawler and Sensor Electronic modules as well as two EMAT sensors were fabricated and assembled for testing as shown in Figure 20.

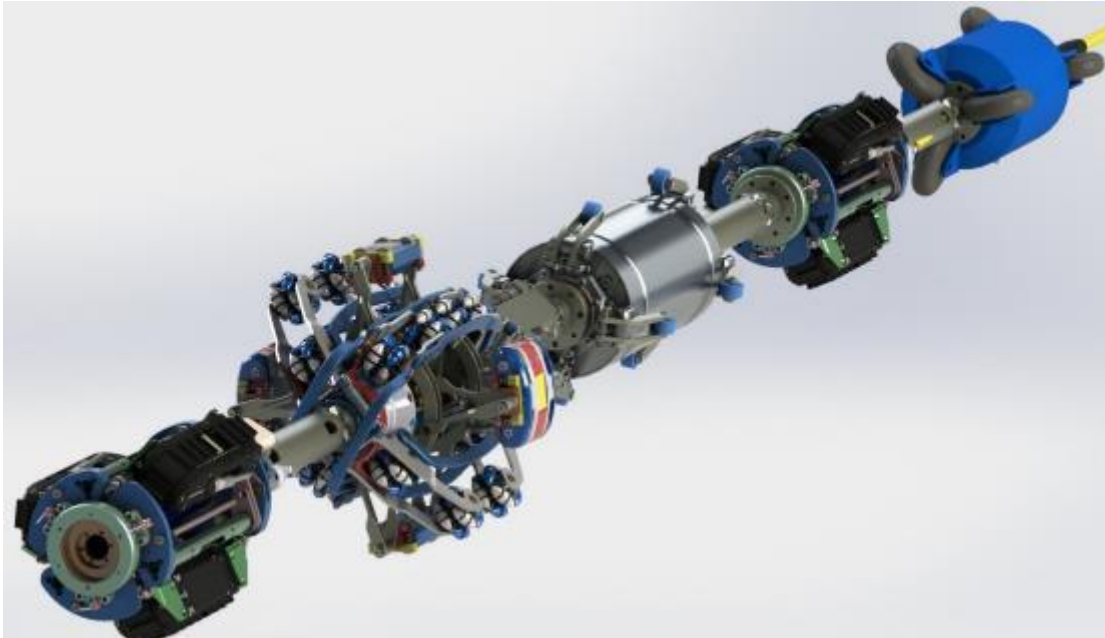


Figure 18. Refined EMAT/PEC Crawler System Design

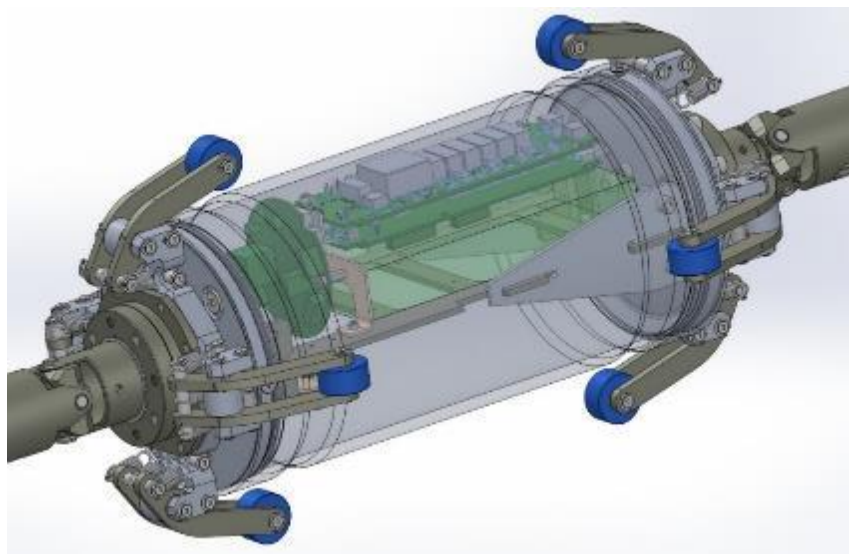


Figure 19. Sensor Electronics Module



Figure 20. Assembled EMAT/PEC and Electronics Sensor Module

Preliminary Testing

The EMAT/PEC subassembly was powered up by Inuktun to assess its performance. The device was tested inside an 8" acrylic pipe for rotation (Figure 21) and on an 8" steel pipe for extension/retraction and rotation (Figure 22). During these testing sessions, Inuktun identified some interferences between parts, the motors needed to be upgraded and the centering mechanism optimized.

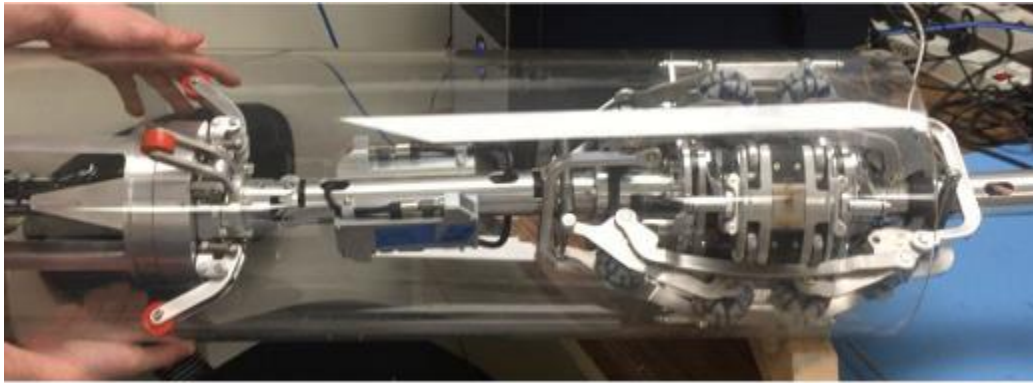


Figure 21. Images of the EMAT/PEC Sensor Module Rotation inside of an 8" Acrylic Pipe.



Figure 22. Views of the EMAT/PEC Sensor Module Rotating inside an 8" Steel Pipe

Mechanical Rework

Based on the testing feedback, the scanner centering mechanism was revised as illustrated in Figure 23. It is important to note that the system underwent four major redesign efforts to ensure the EMAT sensors performed as expected. The system was finally fabricated and assembled.

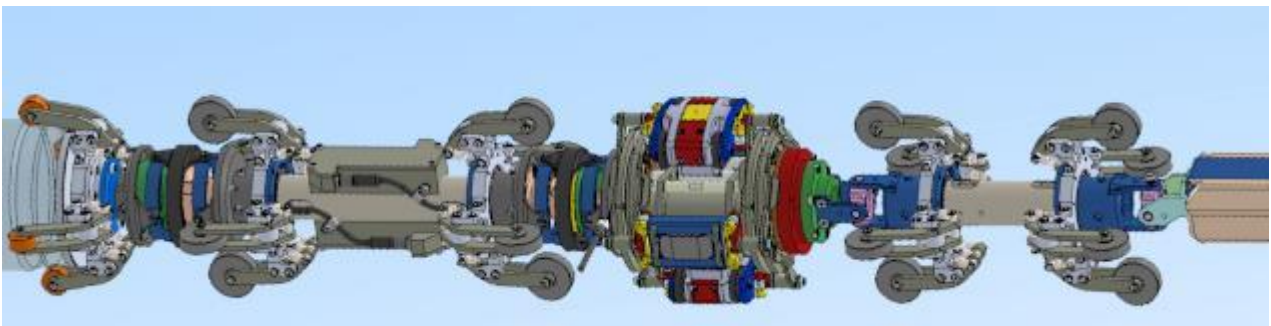


Figure 23. Optimized Centering Mechanism for Scanner

Tool Deployment Considerations

The EMAT/WT tool can be deployed in any orientation (horizontal to vertical). However, we do not want to negotiate a 90-degree 1.5D bend at the insertion point, so a vertical insertion approach cannot be used at this time. However, an initial 45-degree 2D bend should be OK. This initial bend will reduce the maximum number of “bend-degrees” that the tool can navigate in the pipeline section. Similar to a wireline tool, the combined tool and umbilical will be limited by the maximum total bend-degrees due to friction forces acting on the umbilical. We estimate this to be 270 degrees.

The tool also requires sufficient access at the pipeline launch side for insertion and to place an insertion tray at front of the line either in line with the pipe end or at a maximum of 45 degrees from the pipe end. The angled insertion will help shorten the area of excavation a bit. An umbilical spool and computer base station will be located near the entry. The length of the tool is 12 ft. The excavation length will depend on the depth of the line. The pipe entry point needs a welded #150 flange or to be attached to a pipe section with a welded #150 flange for fitting a reducer to get the tool into the pipeline.

Thanks to the long umbilical (1000m), the EMAT/WT system can navigate to a given area of interest to perform a desired wall loss inspection. Since the back of the tool is exposed to the open atmosphere, the line needs to be isolated. Cleaning will be required to assure good sensor contact to the surface and to reduce wear and/or damage to the tool. The tool is equipped with cameras, so potential obstructions or areas of debris can be seen, and the tool stopped. The cleaner the line, the less like an inspection would have to be aborted. These aspects, among others, will be analyzed and discussed with potential pipeline operators during a pre-job assessment to ensure a successful inspection.

SHOP TESTING

The robot was completed, tested, and delivered by Inuktun earlier in Q3/19 to Qi2. The EMAT/WT sensors and electronics were mounted and tested. The completed system was tested for functionality. A pipe with artificial wall loss flaws was inspected with the system and its signals were used successfully to produce C-Scans.

EMAT Sensor/Electronics Integration

The EMAT sensors were integrated into the Sensor Module for signal evaluation. The extension/retraction and rotation mechanisms on this module were connected to a controller provided by Inuktun. The tool subassembly was setup inside an 8" diameter schedule 40 steel pipe as can be observed in Figure 24. Once in place, the extension/retraction mechanism was activated to push the EMAT sensors against the ID pipe surface. An image of an EMAT sensor near the pipe wall is shown in Figure 25. The pulser, receiver, diplexer, and communication boards were mounted and integrated on a frame (E-cage) inside the Electronics Module. During this integration, some grounding and noise issues were identified and solved. The full subassembly (Sensor and Electronics Modules) is shown in Figure 26.



Figure 24. EMAT/WT Subsystem Connected to a Handheld Data Acquisition Unit

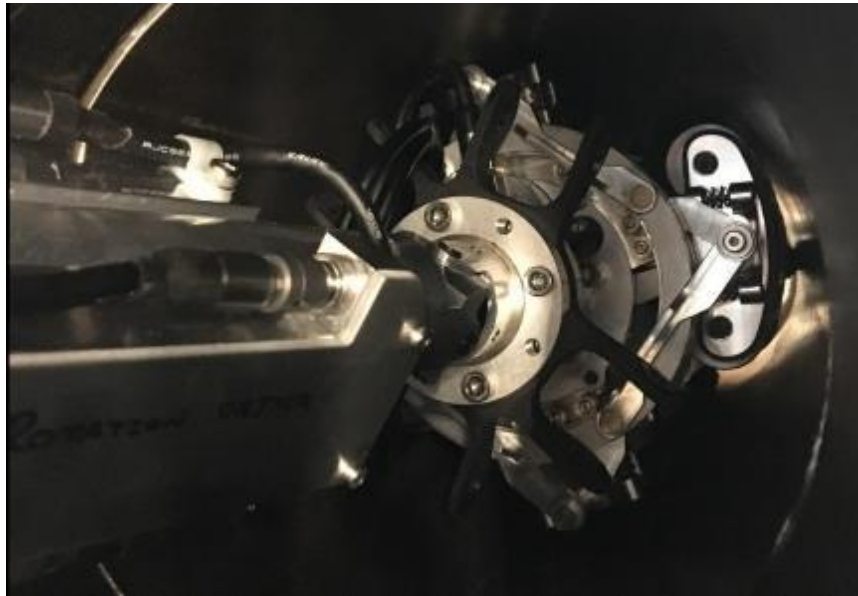


Figure 25. Scanner inside a Pipe



Figure 26. System on Testing Fixture

Some views of the scanner inside the pipe and with the EMAT sensors under rotation are shown in Figure 27. The red arrows are for sensor #1 and the green arrows for sensor #2. Sensor #1 and #2 are placed 180 deg apart. It can be observed that during the scan, the EMAT sensors maintained a full contact against the pipe surface. Acoustic responses were gathered with the on-board electronics for both channels and typical A-Scans for are depicted in Figure 28. The sensors were able to gather multiple reflections (wall echoes) from the pipe. To assess the 360deg inspection, the sensors scanned an ERW pipe with two fabricated wall loss flaws. Thus, B-Scans were produced for both sensors and are presented in Figure 29. On this figure, the ERW zone as well as the flaws are clearly observed!

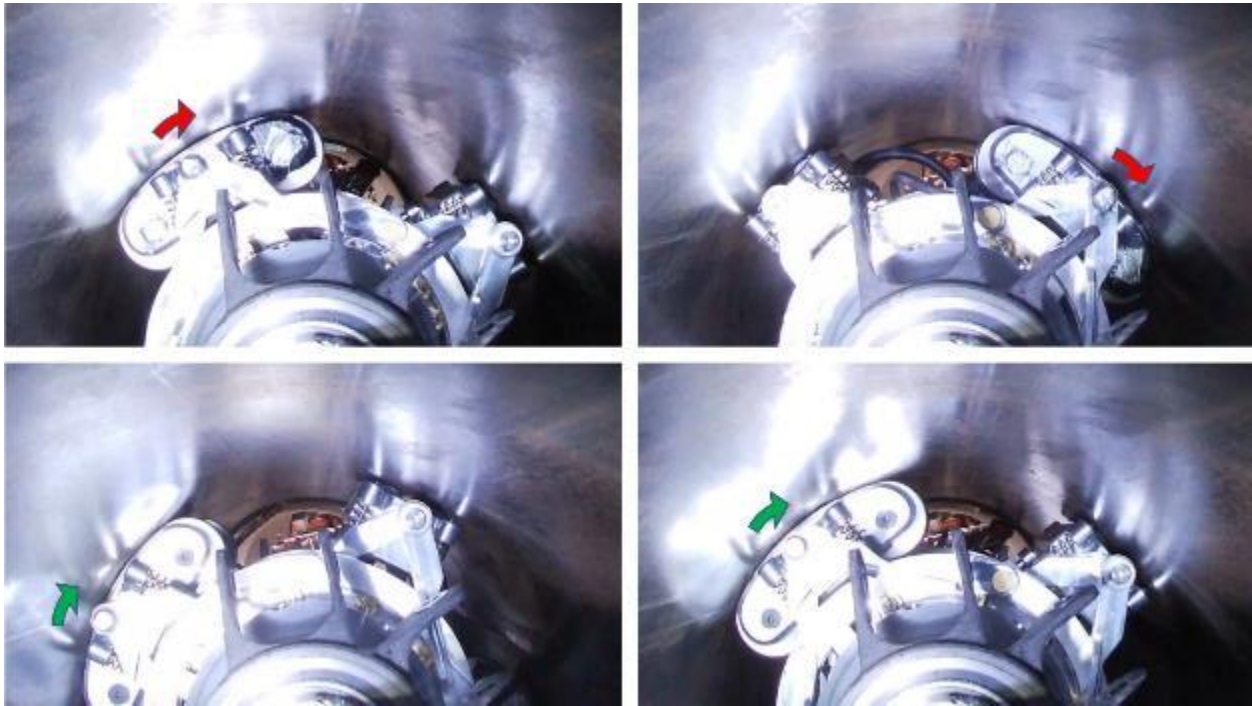


Figure 27. Rotor Scanner with EMAT Sensors Inside a Pipe

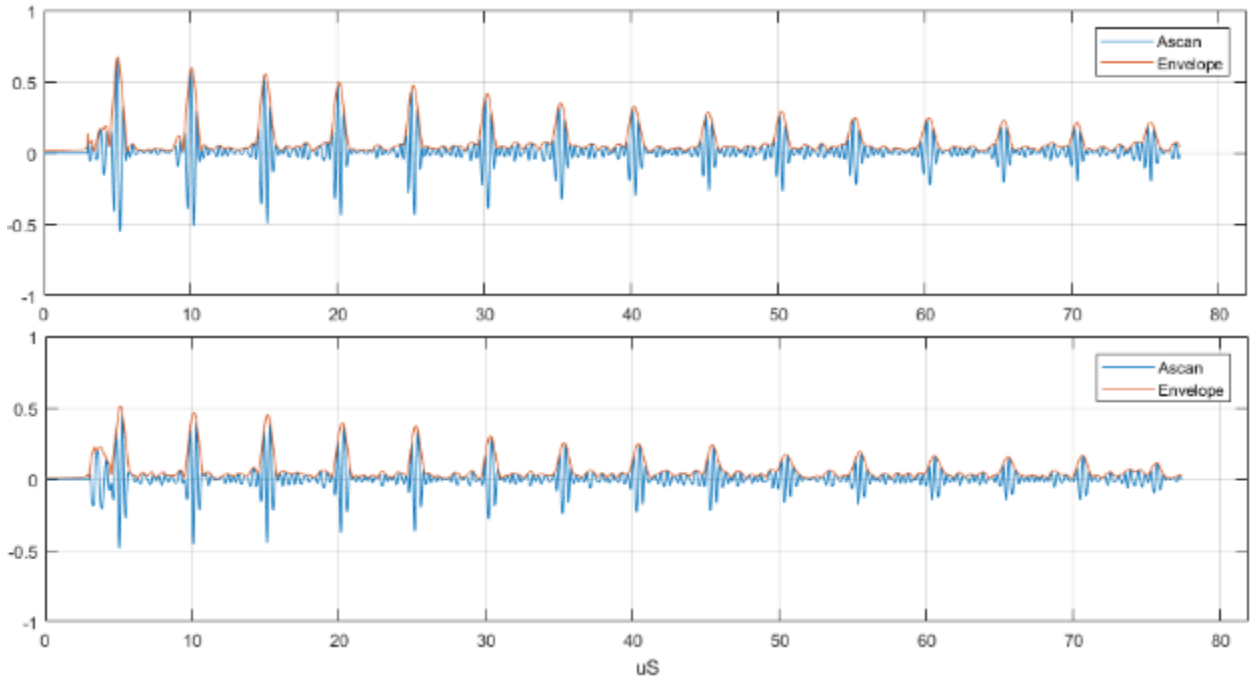


Figure 28. A-Scan of EMAT Sensors 1 and 2 at ping #5.

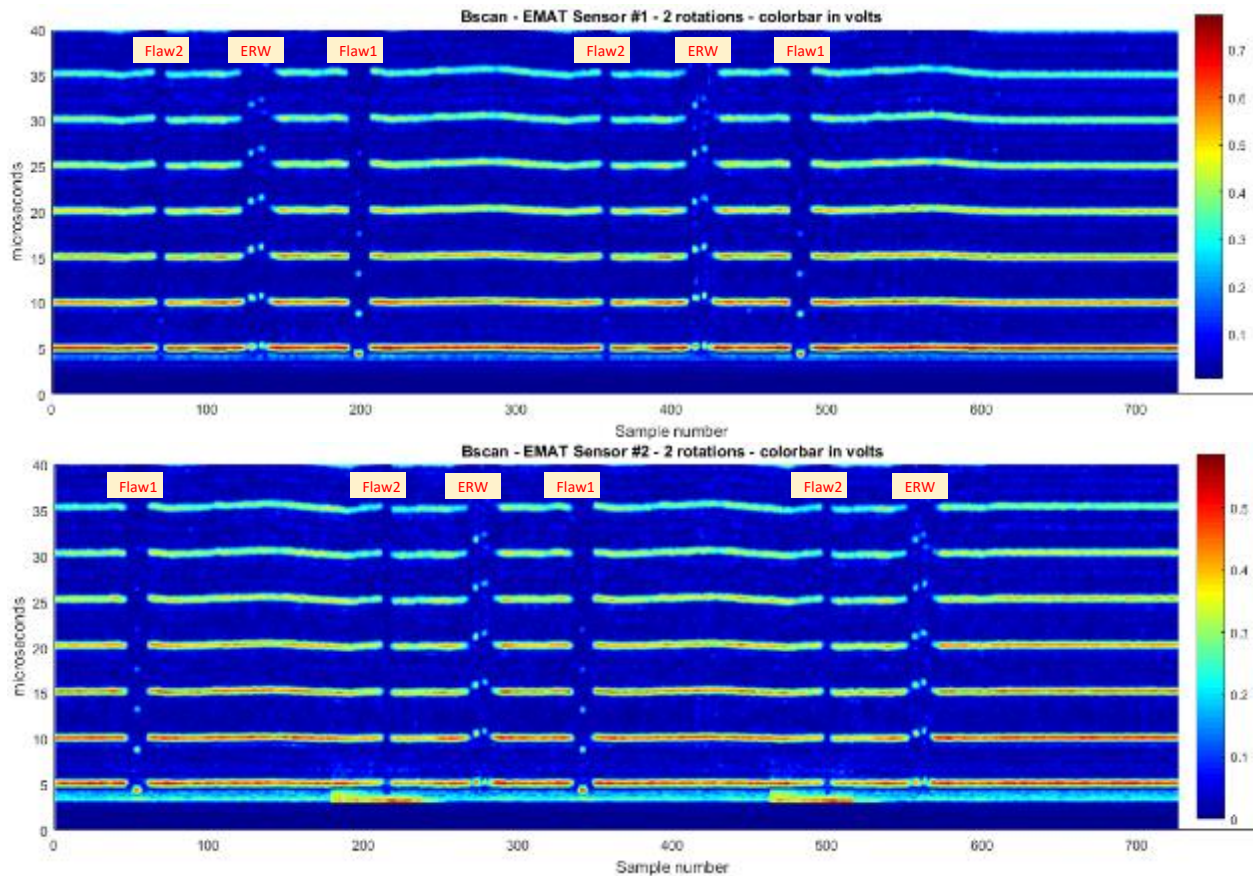


Figure 29. B-Scans for EMAT Sensors 1 (top) and 2 (bottom) Showing Pipe Features

Robotic System Testing

The robot crawler and scanning sensor mechanism were assembled and tested by Inuktun. During earlier preliminary testing, we identified some part interferences, cable routing conflicts, connector positions, and potential issues with the centering mechanisms. Inuktun redesigned some parts and reworked some components to solve the issues. Qi2 verified the recommended design changes and wiring corrections by powering the tool up and performing a preliminary navigation inside of a horizontal 8" diameter steel pipe. The EMAT Wall loss tool has a length of 12ft and can be observed in Figure 30. A 1000m tether and the system base station (computer + power supply) are shown in Figures 31 and 32 respectively. A screen shot of the Graphic User Interface (GUI) that controls the crawlers and scanner is shown in Figure 33. The GUI displays the front and rear cameras for navigation, extension/retraction of the EMAT/PEC sensors and setting the system speeds. The software includes some bottoms and boxes to set the rotational and translational scanner speeds to ensure a 100% inspection coverage.



Figure 30. EMAT/Wall Loss tool



Figure 31. EMAT/Wall Loss Tether



Figure 32. Base Station



Figure 33. Base Station Graphic User Interface

In-House Testing

Once the robotic platform arrived at Qi2, we reconnected the EMAT sensors and associated electronics with the rest of the system. An image of the integrated tool is shown in Figure 34. For testing, we used our 8" schedule 40 pipe section with nominal all thickness of 0.322" and artificial flaws (See Figure 11). After several small modifications and tests, the system went alive. A view of the base station computer showing the sensors inside the pipe as well as live EMAT signals are shown in Figure 35. A detailed view of the gathered acoustic responses (multiple echoes) for both sensors are presented in Figure 36.

The pipe was scanned using different settings to assess difference in behavior and C-Scans were produced as the one shown in Figure 37. In this figure can be observed that the flaws were clearly identified and thanks to the high resolution of our EMAT sensors, measurements were taken on those flaws. It is important to note that the flaws in the test sample were created using a ball end mill or milled flat (tangent). This means that in both cases there is only a single axial line where the tangent of the flaw is parallel to the inner surface of the pipe. This is the most critical test. Most wall loss test samples are created by machining the bottom of the flaws parallel to the inside surface for at least the length of the sensor resolution making the flaws easier to characterize. The long diagonal "green" line along the C-Scan is the ERW line. It is important to note that two narrow EDM notches, to simulate cracks, were present on the sample. These flaws were also detected as long and narrow bands below the square and round flaws

The C-scan plot represents a solid and successful integration between the EMAT sensors, EMAT electronics, the robotic platform as well as the communication along the system and processing of the signal. The high resolution of the 1/4" measurement foot-print EMAT sensor was clearly demonstrated.



Figure 34. Integrated EMAT/WT Robotic System



Figure 35. Robot Base Station (left) and EMAT Signals (right)

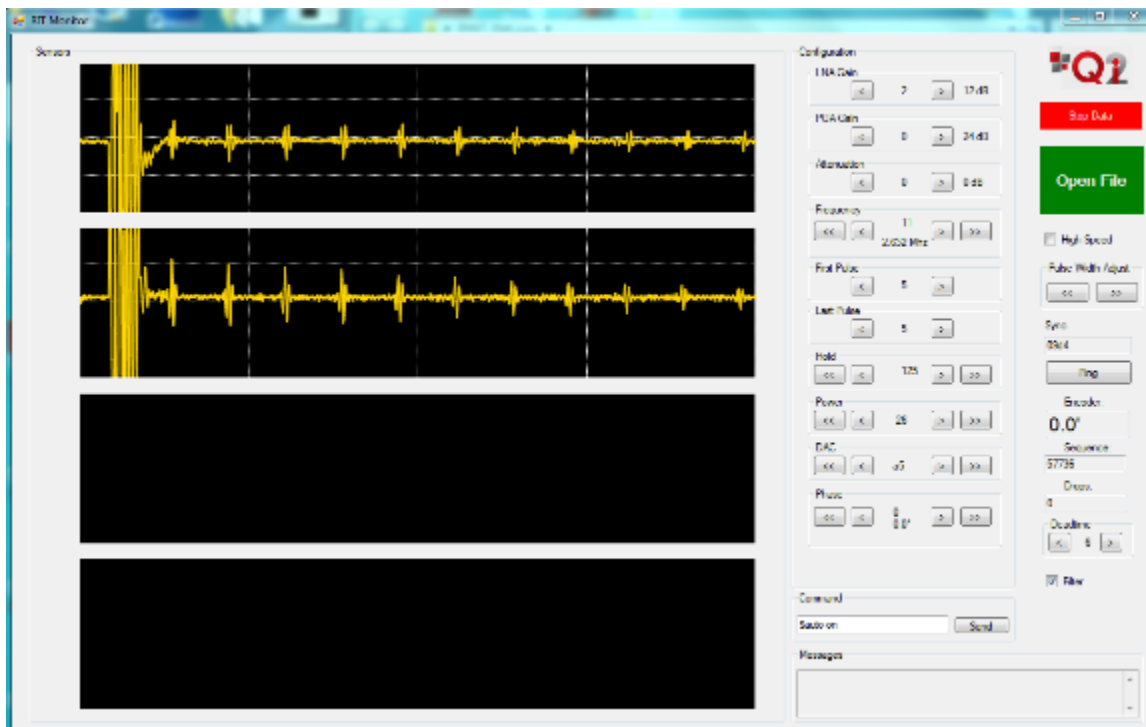


Figure 36. EMAT/WT Signals from the System

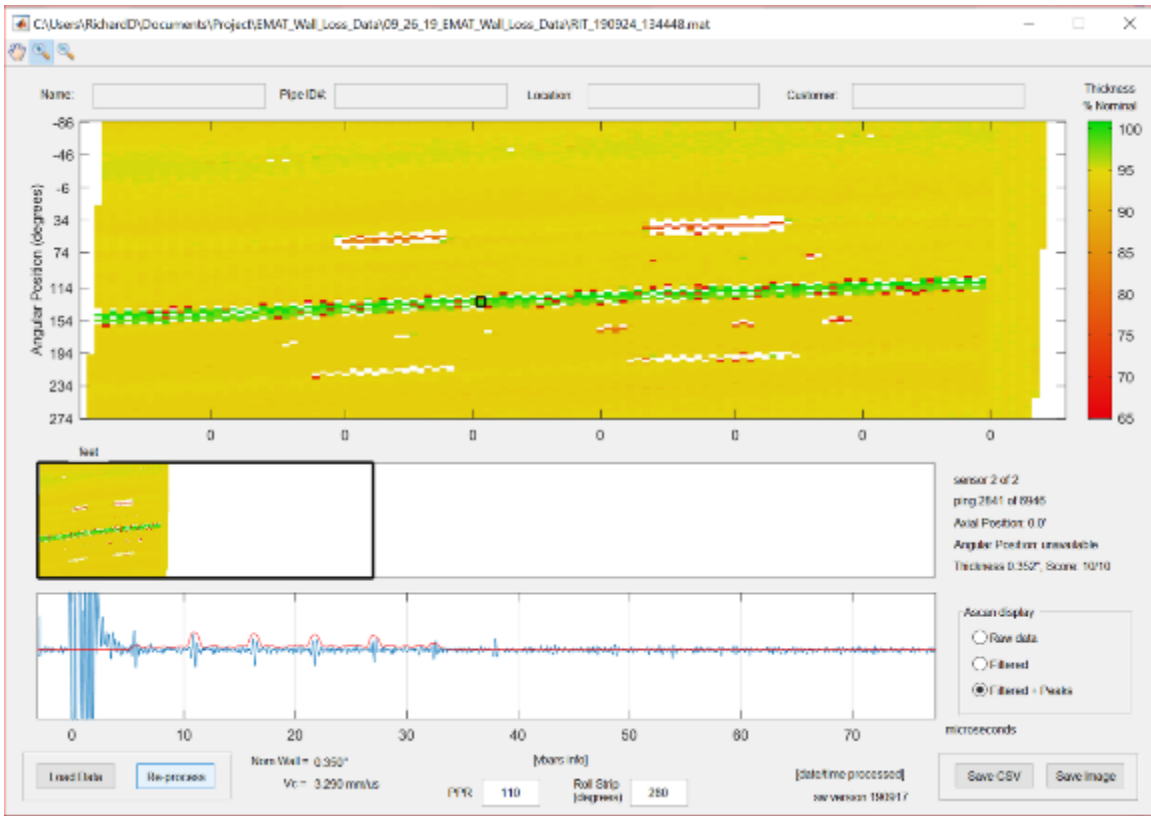


Figure 37. EMAT C-Scan using One Cycle at 2 RPM

FIELD TESTING

After some additional tweaks on the EMAT/WT system, Qi2 personnel travelled to Q-Inline facilities in La Grange, TX and performed functional field testing on December 17 and 18, 2019. The robotic unit, computer base station, and tether were deployed outdoors next to some piping for testing as shown in Figures 38 and 39 respectively. Three piping setups were used to assess the unit performance and to detect wall loss flaws.



Figure 38. EMAT/WT tool



Figure 39. EMAT/WT Base Station and Tether

Setup 1

A piping setup was assembled with six 8" diameter pipe segments. The segments were attached using bolted flanges with a total length of 116ft. Figures 40 and 41 show the setup and a sketch of the pipe configurations respectively. Two X42 pipes with different schedules and machined metal loss flaw were placed in positions 4 (Sch 40) and 5 (Sch 20). These pipes are normally used by Q-Inline for MFL testing. It is important to note that these flaws have rounded edges as can be observed in Figure 42. A cleaning pig was run through the line to ensure it was free of any debris that could damage the tool.

A PVC "launcher" and a 10"-8" PVC reducer were mounted at one end of the setup as an insertion bed for the robot (Figure 43). The EMAT/WT system was powered up and the crawler navigated through the pipes 1-3 with the scanning mechanism retracted. Once the tool reached pipe 4 (i.e. first metal loss pipe), the scanning mechanism was extended and rotated at 31 RPM to collect wall thickness data. Live signals from the sensors are shown in Figure 44. After scanning the pipe for ~ 6ft, unfortunately one of the EMAT signals was lost, as a result, the inspection was stopped. The tool was extracted from the pipe for further assessment. It was found that one of the wear pads was damaged probably during tool navigation. The second wear pad was found ok. The data was processed and produced a C-Scan of the inspected pipe section as shown in Figure 46. It can be observed that the tested pipe has a wide variation on wall thickness. Q-Inline indicated that the pipes, at position 4 and 5, were very noisy due to very poor manufacturing quality. Nevertheless, the EMAT/WT was able to measure wall thicknesses on many places on the pipe including on the bottom of some medium/large machined metal loss flaws. The system was also able to provide a picture of the shapes of those flaws.



Figure 40. Piping Setup 1



Figure 41. Setup 1 Pipeline Detail



Figure 42. Detailed view of Pipe with Metal Loss Flaws on Setup 1



Figure 43. EMAT/WT Robot Deployment on Setup 1

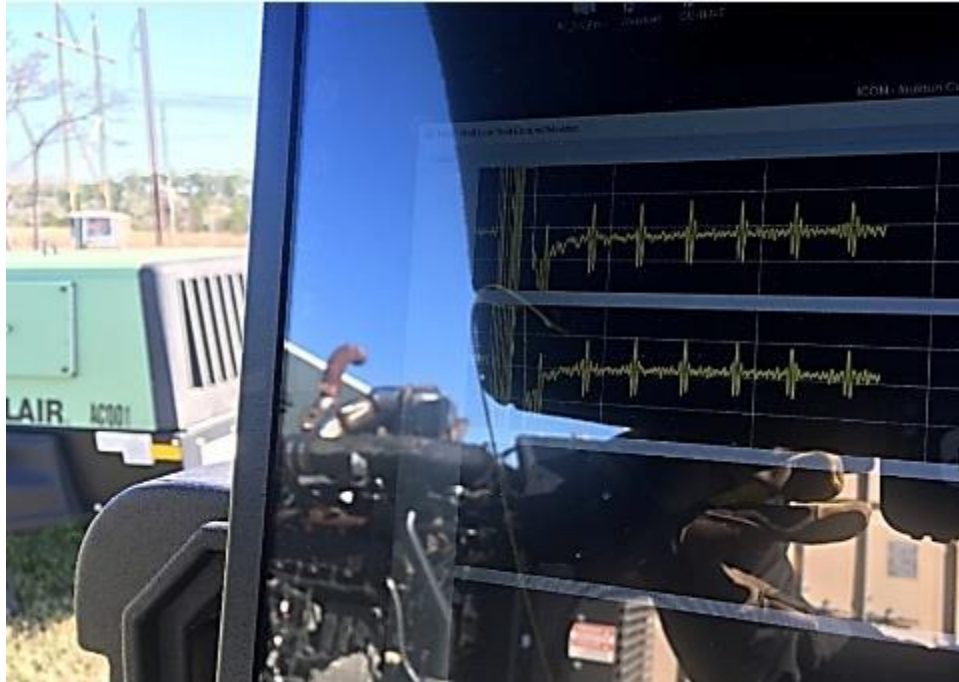


Figure 44. EMAT/WT Ultrasonic A-Scan Responses During Inspection on Setup 1

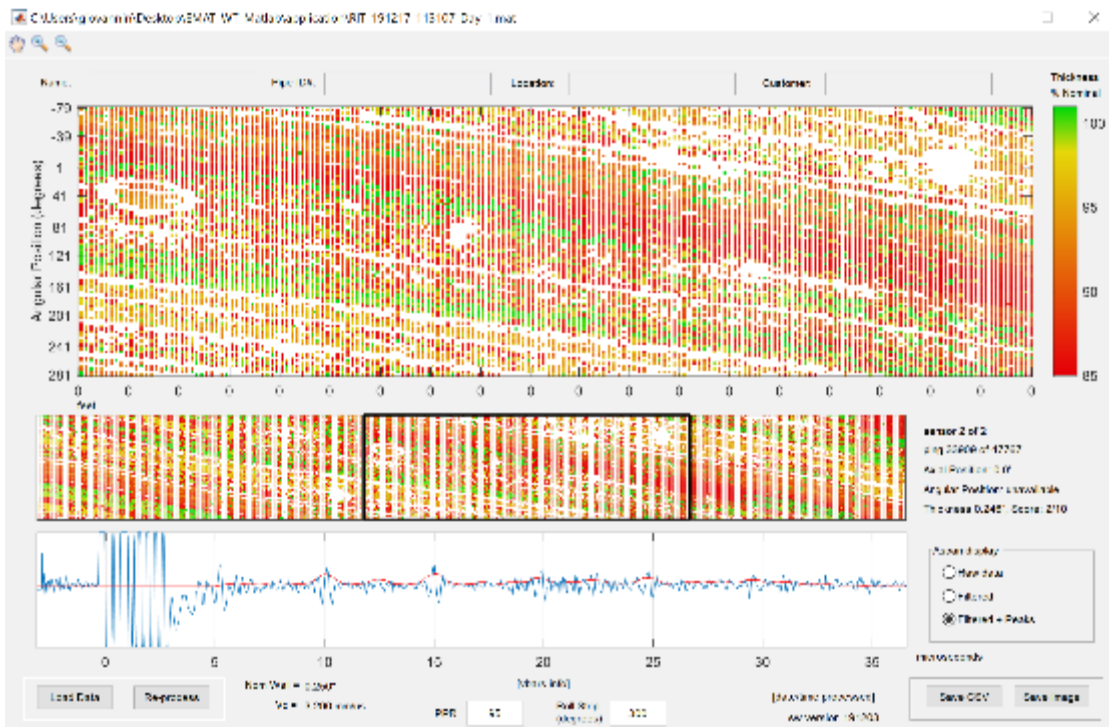


Figure 46. EMAT C-Scan for Pipe in Setup 1 at 31 RPM

Setup 2

After replacing the broken wear pad, a different piping setup was used to avoid any further damage on the pads. An X42 8" diameter pipe with a total length of 42.9ft and schedule 20 was selected. The tool was guided into the pipe using a 10"-8" steel reducer (Figure 47). Some metal loss flaws on the pipe can be observed in Figure 48 with a detailed flaw map depicted in Figure 49 and specs in Table1. The EMAT/WT robot was inserted into the pipe (Figure 50) to perform an EMAT inspection with live signals shown in Figure 51. Some views of the robot inside the pipe as well as the other end of the pipe are shown in Figures 52 and 53 respectively. Once the scan was completed in the *forward* direction, the robot crawled back collecting data again (*backward* direction), and it was removed from the pipe. The wear pads were inspected and found functional without any apparent damage. C-Scans were produced for both scanning directions and are presented in Figure 55 for forward and Figure 56 for backward directions. On the forward C-Scan, we can observe that the EMAT/WT scanner was able to detect 40 of the 42 flaws! The 2 missed flaws were probably too narrow for the sensor to be detected. On the backward C-Scan, of Figure 56, can be noted that the data is a bit noisier than on the forward C-Scan (Figure 55). This was due to an accidental increase in axial velocity of the robot during scanning. In spite of that incident, the superior quality of the pipe in Setup 2, in comparison with those used on Setup1, is evident in both C-Scans. Furthermore, the flaw shapes are almost well-defined in most of the cases due to acoustic signal losses on their rounded edges. Finally, the system was able to get wall thickness measurements at the bottom of some flaws for the given radial and axial scanning speeds. It is clear that a more detailed C-Scan of the pipe can be obtained by reducing the scanning speed.



Figure 47. Piping Setup 2 with EMAT/WT Robot Deployed



Figure 48. Detailed view of Pipe with Metal Loss Flaws on Setup 2

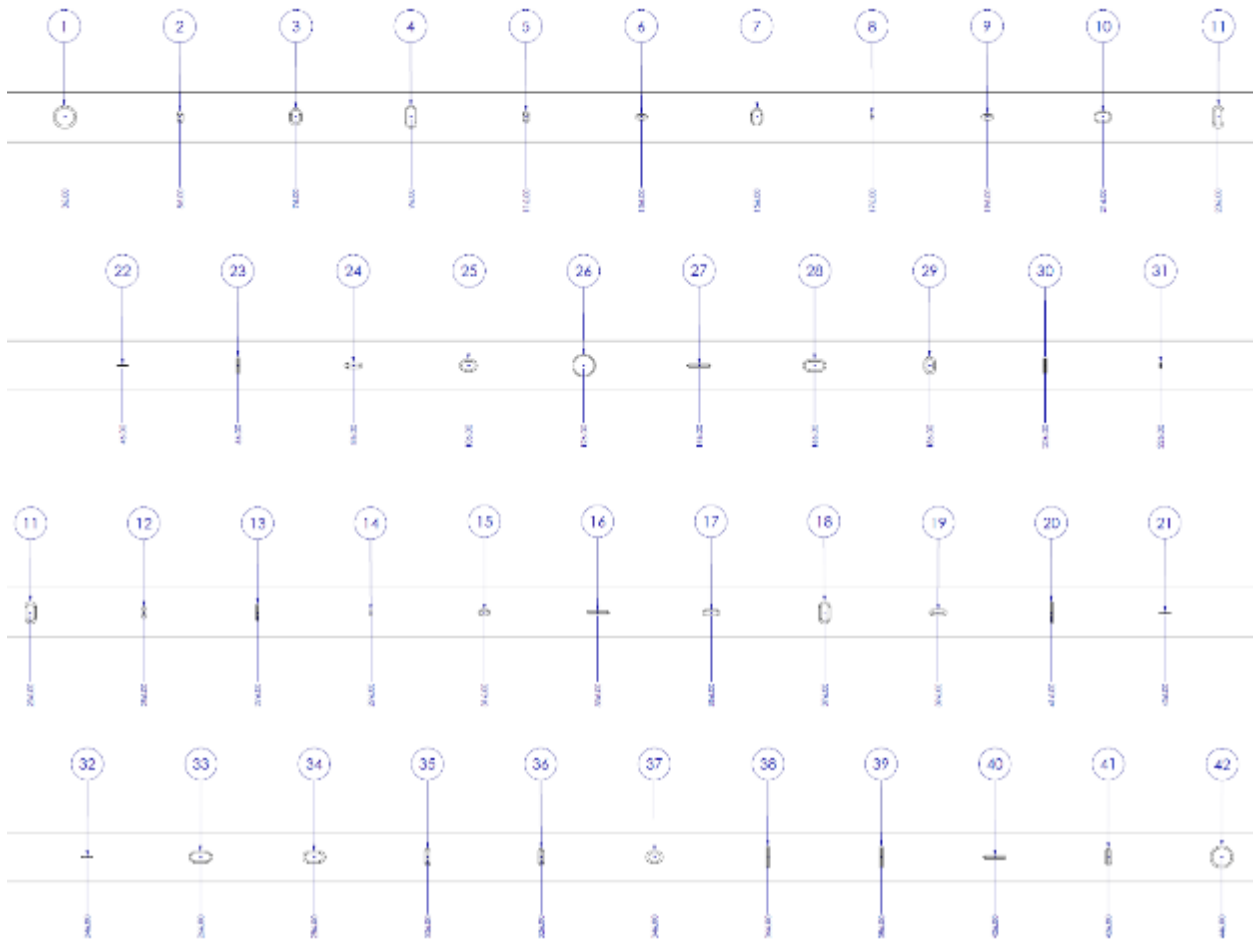


Figure 49. Metal Loss Flaw Map for Pipe on Setup 2

DEFECT	LENGTH	WIDTH	DEPTH	DEPTH (%)	Nom. Bit Diameter	Orientation	Position
1	4.00	4.00	0.188	75	1.00	90	36.0
2	1.00	2.00	0.125	50	1.00	90	56.0
3	2.00	3.00	0.125	50	1.00	90	76.0
4	2.00	4.00	0.063	25	1.00	90	96.0
5	1.00	2.00	0.063	25	1.00	90	116.0
6	2.00	1.00	0.125	50	1.00	90	136.0
7	2.00	3.00	0.063	25	1.00	90	156.0
8	0.25	1.00	0.188	75	0.25	90	176.0
9	2.00	1.00	0.188	75	1.00	90	196.0
10	3.00	2.00	0.063	25	1.00	90	216.0
11	2.00	4.00	0.188	75	1.00	90	236.0
12	1.00	2.00	0.188	75	1.00	90	256.0
13	0.50	3.00	0.063	25	0.50	90	276.0
14	0.25	1.00	0.125	50	0.25	90	296.0
15	2.00	1.00	0.063	25	1.00	90	316.0
16	4.00	0.50	0.125	50	0.50	90	336.0
17	3.00	1.00	0.063	25	1.00	90	356.0
18	2.00	4.00	0.125	50	1.00	90	376.0
19	3.00	1.00	0.188	75	1.00	90	396.0
20	0.50	4.00	0.063	25	0.50	90	416.0
21	2.00	0.25	0.125	50	0.25	90	436.0

DEFECT	LENGTH	WIDTH	DEPTH	DEPTH (%)	Nom. Bit Diameter	Orientation	Position
22	2.00	0.25	0.063	25	0.25	270	46.0
23	0.50	3.00	0.125	50	0.50	270	66.0
24	3.00	1.00	0.125	50	1.00	270	86.0
25	3.00	2.00	0.125	50	1.00	270	106.0
26	4.00	4.00	0.063	25	1.00	270	126.0
27	4.00	0.50	0.063	25	0.50	270	146.0
28	4.00	2.00	0.125	50	1.00	270	166.0
29	2.00	3.00	0.188	75	1.00	270	186.0
30	0.50	3.00	0.188	75	0.50	270	206.0
31	0.25	1.00	0.063	25	0.25	270	226.0
32	2.00	0.25	0.188	75	0.25	270	246.0
33	4.00	2.00	0.063	25	1.00	270	266.0
34	4.00	2.00	0.188	75	1.00	270	286.0
35	1.00	3.00	0.188	75	1.00	270	306.0
36	1.00	3.00	0.125	50	1.00	270	326.0
37	3.00	2.00	0.188	75	1.00	270	346.0
38	0.50	4.00	0.125	50	0.50	270	366.0
39	0.50	4.00	0.188	75	0.50	270	386.0
40	4.00	0.50	0.188	75	0.50	270	406.0
41	1.00	3.00	0.063	25	1.00	270	426.0
42	4.00	4.00	0.125	50	1.00	270	446.0

Table 1. Metal Loss Flaw Specs for Pipe from Figure 12



Figure 50. Back of EMAT/WT Robot inside Pipe of Setup 2

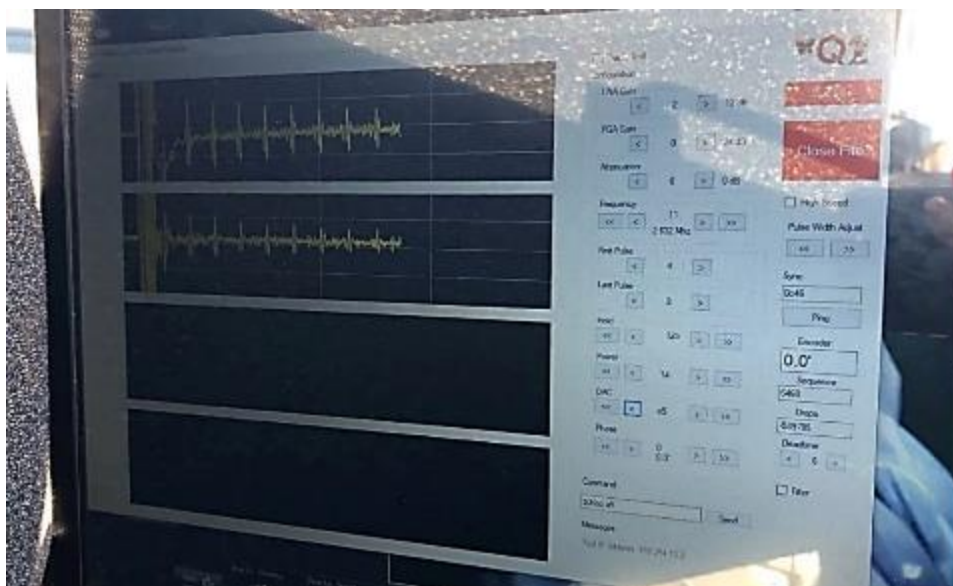


Figure 51. EMAT/WT Ultrasonic Responses During Inspection on Setup 2

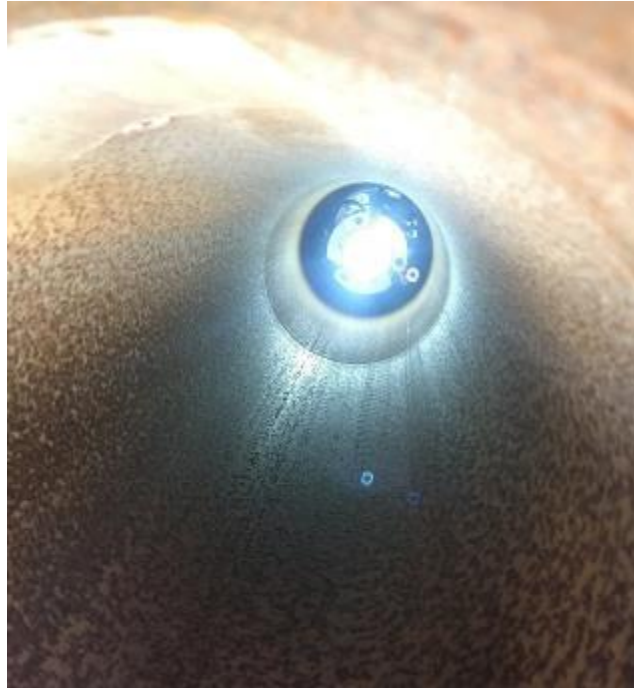


Figure 52. Front View of EMAT/WT Robot inside Setup 2



Figure 53. EMAT/WT Robot at the end of Setup 2

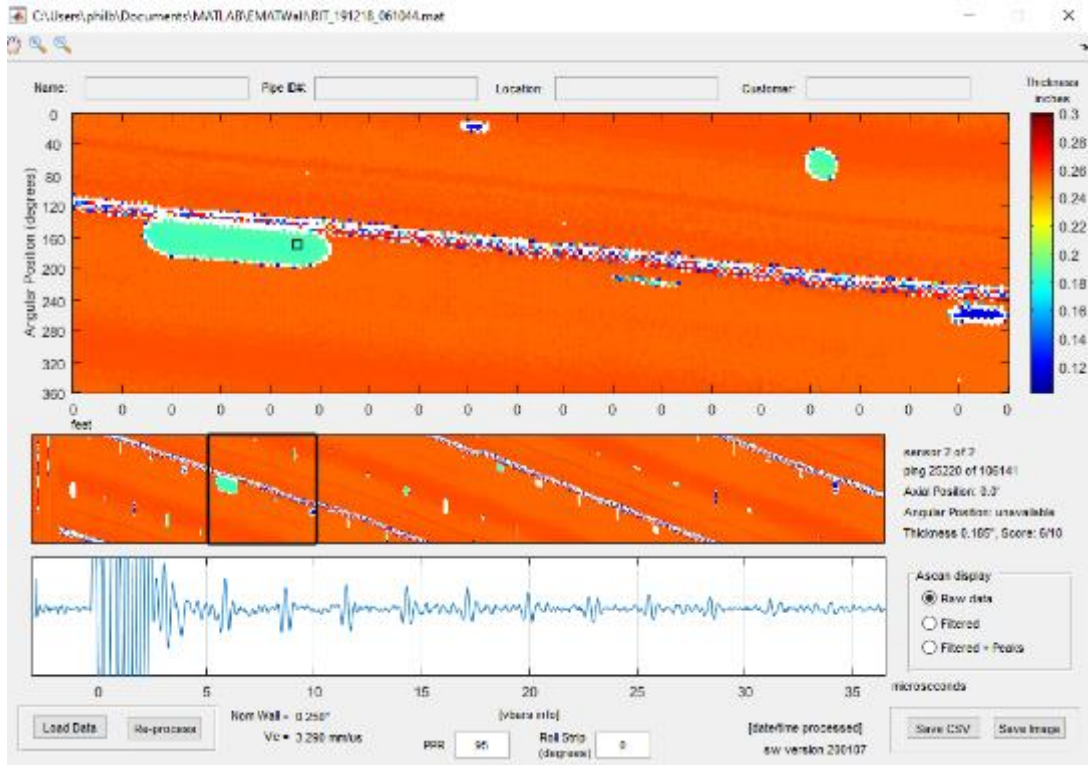


Figure 55. EMAT C-Scan for Pipe in Setup 2 on Forward Direction at 31 RPM

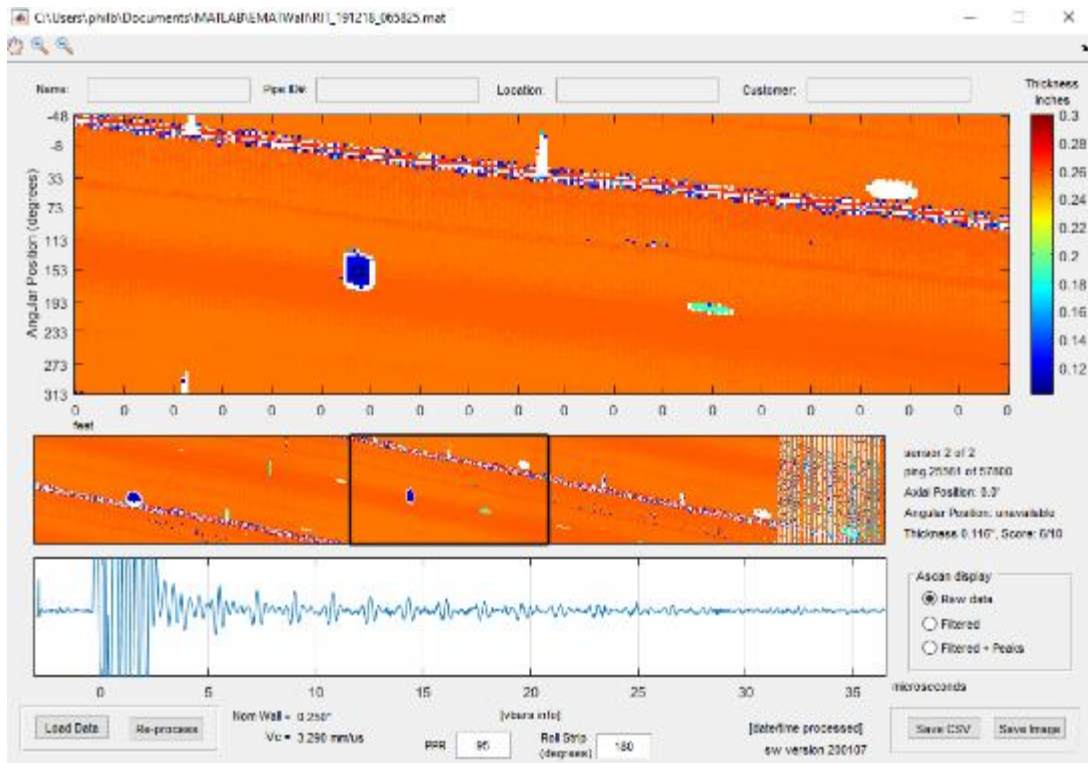


Figure 56. EMAT C-Scan for Pipe in Setup 2 on Backward Direction at 31 RPM

Setup 3

Thanks to the good results obtained by the EMAT/WT system on the Setup 2, we decided to return and scan the pipes with metal loss flaws from Setup 1. These pipes were moved to a separate area and a reducer was installed at one of its help with the robot navigation. The new setup can be observed in Figure 57. Figure 58 shows the metal loss flaws on one of the pipes. These X42 pipes have two different schedules: Sch 20 for the first pipe after the reducer, and Sch 40 for the second pipe on the setup. The EMAT/WT tool before deployment is shown in Figure 59. Once the scanning head was inside the pipe and the tool body provided good support for the scanner, the inspection was started. On the first run, the robot scanned both pipes and the C-Scan result is presented in Figure 60. A second run or inspection was performed while the robot was returning to its starting position (i.e. backwards). The resulting C-Scans on this run are shown in Figures 61 and 62. It can be noted that one of the EMAT sensors has a lower sensitivity than the other one. Also, the scanner motors are too noisy reducing the signal-to-noise ratio on both sensors. We will reduce that noise in the future. On these C-Scans can be observed that both pipes have different material qualities. The first pipe is the same one with low quality scanned on Figure 46. In addition, the difference in wall thicknesses on both pipes is evident. It is important to note that our software application was designed to analyze only one wall thickness at the time. A future version of the software needs to be able to handle multiple pipe materials and wall thicknesses. Once the tool was extracted, the wear pads were inspected and found in good conditions. It is clear that for longer runs, the EMAT Sensor module design needs to be improved based on ceramic wear pads and to make easier for it to pass between different pipes.



Figure 57. Piping Setup 3



Figure 58. EMAT FWD C-Scan for Pipe in Setup 3



Figure 59. EMAT/WT Robot Deployment on Setup 3

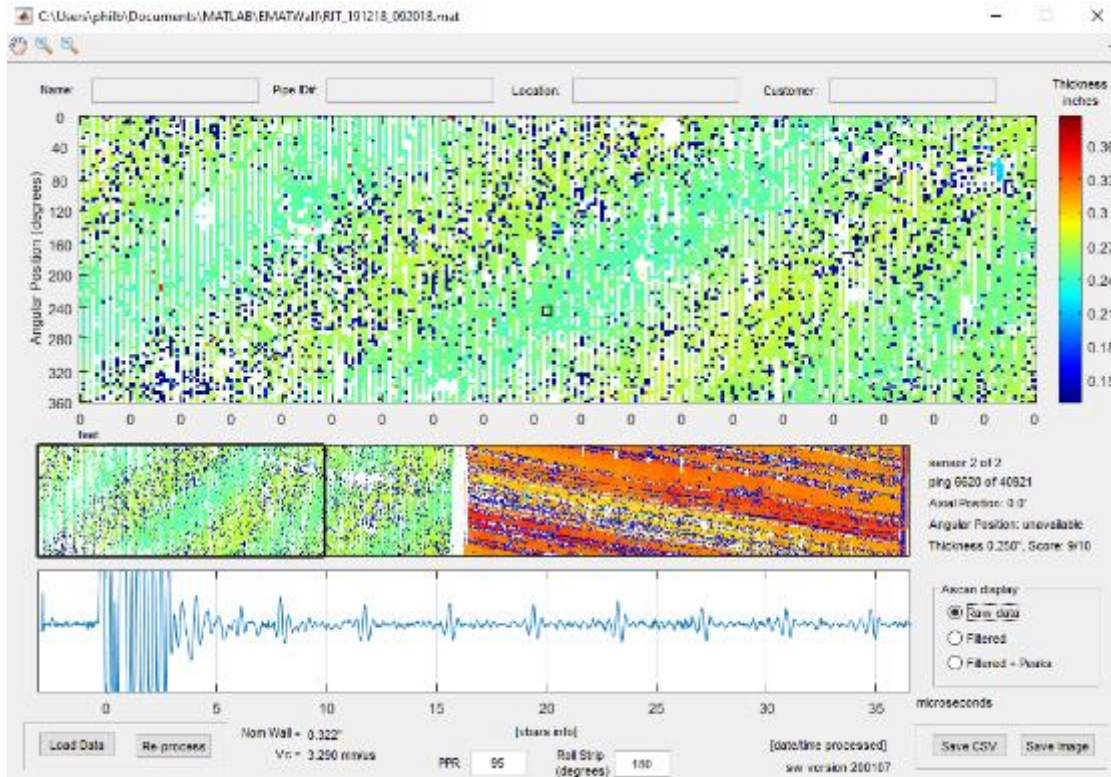


Figure 60. EMAT C-Scan for Pipe in Setup 3 on Forward Direction at 31 RPM

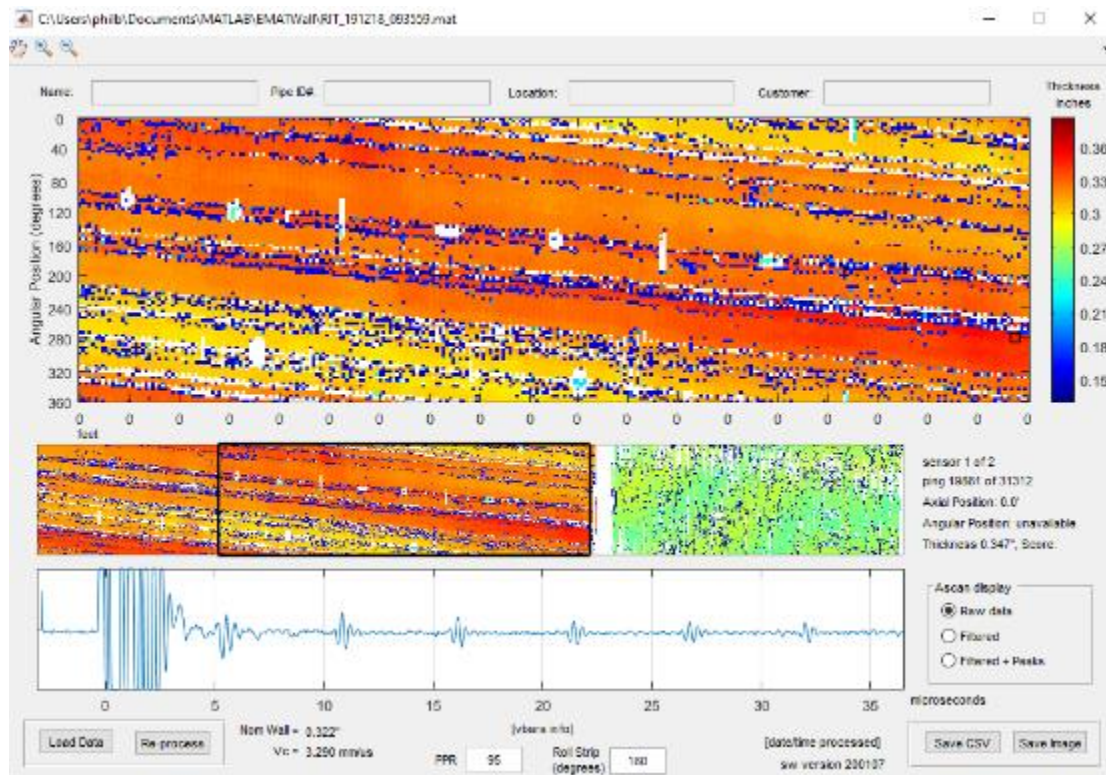


Figure 61. EMAT C-Scan for Pipe in Setup 3 on Backward Direction at 31 RPM

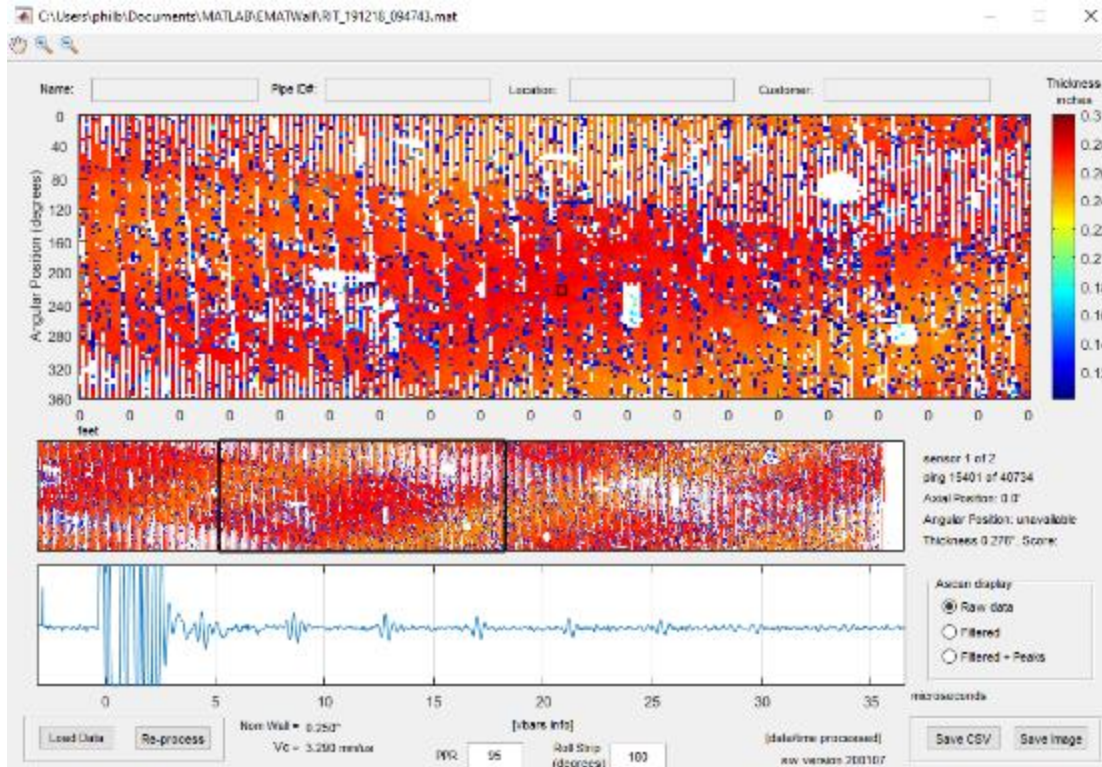


Figure 62. EMAT C-Scan on Last Section for Pipe in Setup 2 on Backward Direction at 31 RPM

CONCLUSIONS AND FUTURE WORK

An electromagnetic acoustic transducer (EMAT) sensor-based robotic system was successfully developed and field-tested. The EMAT sensor was specifically designed to directly measure the remaining wall thickness. Different concepts were studied producing a 1/4" footprint EMAT sensor that could be integrated on multiple pipe inspection platforms. A patent application was filed for this novel design. The tool was designed to assess 8"-12" diameter unpiggable pipelines containing reduced diameter fittings and other restricting features. The development work included not only sensor configurations but also custom electronics, scanning mechanisms, and custom robotic platform among others. Firmware was coded to drive the electronics and software to process the data and created C-Scans. The sensors were tested on flat plates, curved samples, pipe sections and ultimate, pipe strings on the field. A-Scans, B-Scans, and C-Scans were computed for the EMAT sensors at different stages of the project.

Based on the field-test results, it is clear that the system still needs some further refinements. Sensor wear pads will be upgraded to ceramic-based ones to increase their durability. The EMAT sensor carrier needs to be fine tuned to improve the transition between pipes as a result, wear pad durability will increase. Regarding sensor performance, noise produced by the electrical motors of the scanning mechanisms need to be minimized. This will improve the signal-to-noise ratio of the EMAT sensors considerably and should significantly increase the amount of good C-Scan data in the noisy pipe sections, Figures 60 through 62 and marginal areas in Figures 55 and 56.

Finally, full integration of the Pulse Eddy Current (PEC) sensors needs to be complete. This EMAT/PEC sensor suite will make the tool more robust and ready to go to commercialization.